Original article

Characterization and phytochemical constituents of Periploca hydaspidis Falc crude extract and its anticancer activities

Saima Ali [a], Muhammad Rashid Khan [a,*], Riffat Batool [a], Sayed Afzal Shah [b], Javed Iqbal [c,*], Banzeer Ahsan Abbasi [d], Tabassum Yaseen [c], Nida Zahra [d], Adil Aldhahrani [e], Fayez Althobaiti [f]

[a] Department of Biochemistry, Faculty of Biological Sciences, Quaid-i-Azam University, Islamabad 45320, Pakistan
[b] Department of Biological Sciences, National University of Medical Sciences, Rawalpindi, Pakistan
[c] Department of Botany, Bacha Khan University, Charsadda, Khyber Pakhtunkhwa, Pakistan
[d] Department of Plant Sciences, Quaid-i-Azam University, Islamabad 45320, Pakistan
[e] Clinical Laboratory Sciences Department, Turabah University College, Taif University, Taif 21995, Saudi Arabia
[f] Department of Biotechnology, College of Science, Taif University, P.O. Box 11099, Taif 21944, Saudi Arabia

A B S T R A C T

The current study aims to investigate the anticancer potential of Periploca hydaspidis extracts against HCCLM3 and MDA-MB 231 cell lines with invasive properties and to identify molecular targets underlying its action mechanism. Cytotoxic screening of plant extracts was done via MTT assay against liver and breast cancer cell lines and GC/MS of the best cytotoxic fraction was performed to identify its chemical composition. Flow cytometry detected apoptosis and cell-cycle changes after drug treatment. The specified cells were studied for migration and invasion potential along with performing western blot analysis of proteins involved in apoptosis, cell-cycle, metastasis, and MAPK (Mitogen-activated protein kinase) cell-signaling pathway. The results revealed the crude methanol (PHM) fraction of P. hydaspidis shown dose and time dependent cell-proliferative inhibition response. GC/MS analysis detected 54 compounds of which fatty acids (29.8%), benzenoids (15.7%), and esters (14.3%) constituted the bulk. The inhibitory effect against cancer cells was linked with cell-cycle arrest at G0/G1 phase, induction of apoptosis, reduced migration and invasion capabilities post treatment. PHM induced apoptosis via downregulation of anti-apoptotic (survivin, B-cell lymphoma Extra-large; BCL-XL, X-linked inhibitor of apoptosis protein; XIAP, Myelocytomatosis; C-myc), metastatic (Matrix metallopeptidases 9/2; MMP9/2), and cell-cycle regulatory (cyclin D1 and E) proteins, whereas upregulation of pro-apoptotic proteins (Bcl-2 homologous antagonist/killer; BAK, Bcl-2-Associate X protein; BAX, cleaved caspases; 3,7,8,9, and PARP) and activation of MAPK (Jun amino-terminal kinase; JNK and P38) pathway. P38 was needed for PHM-induced apoptosis, where the inhibition of P38 by pharmacological inhibitor (SB239063) diminished the apoptotic effects. Overall, our results conclude that PHM can inhibit cell-proliferation and induce apoptotic effects by activation of P38 MAPK cell-signaling pathway. This suggests the methanol fraction of P. hydaspidis (PHM) to have anticancer compounds, potentially useful for treating liver and breast cancer. In future, one-step advance studies of PHM regarding its role in metastatic inhibition, immune response modulation for reducing tumor, and inducing apoptosis in suitable animal models would be an interesting and promising research area.

© 2021 The Author(s). Published by Elsevier B.V. on behalf of King Saud University. This is an open access article under the CC BY-NC-ND license (http://creativecommons.org/licenses/by-nc-nd/4.0/).

1. Introduction

Owing to the morbidity and high mortality rate, cancer is considered a world-wide public health-concern since decades accounting to greater than 9 million in 2018 and 10.0 million death cases in 2020 (Abbasi et al., 2018, Sung et al., 2021). Although, vaccination and lifestyle adjustment is considered the most effective preventive measure in regulating cancer yet, environmental and ageing factor cannot be voluntarily controlled. The list of

ever-growing targeted therapeutics proves that treatment of cancer has taken great strides since the innovation of Tamoxifen in 1970 (Stewart and Wild, 2014). FDA-approved drugs include>50% cancer therapeutics derived from natural sources such as plants, animals, fungi and algae (Batool et al., 2017, Abbasi et al., 2019, Abbasi et al., 2020a). These natural resources hence necessitate the unraveling of novel chemo preventive/chemotherapeutic alternatives with no or less toxicity and side-effects on normal tissue to be a more promising therapeutic window (Iqbal et al., 2018a, Iqbal et al., 2018b, Batool et al., 2019).

Among the different lethal cancers, hepatocellular carcinoma (HCC) is considered as the 5th solid tumor world-wide and the 3rd leading origin of cancer mortality around the globe, accounting for 0.626 million death cases annually (Abbasi et al., 2020b, Abbasi et al., 2021). HCC cases are increasing steadily since past few decades. Majority of the cases are ascribed to underlying infections created by hepatitis B and C virus. Other contributing risk factors involved in its possible etiology include obesity, iron overload, alcohol consumption, several dietary carcinogens i.e. nitrosamines and aflatoxins, and environmental pollutants (Abbasi et al., 2020c, Abbasi et al., 2020d). As the mechanism of HCC aggressive behavior at molecular level still remains unclear, therefore there is an urgent prerequisite to identify new biochemical markers for foreseeing HCC's aggressive biology in addition to improving the availability of present therapeutic strategies for HCC Hashemi, 2015; Zhang et al., 2017). Besides this, the cancer affecting > 1 million women every year globally is diagnosed as breast cancer and is reported as the leading type of cancer in women (Najmuddin et al., 2016). It is characterized as estrogen-receptor (ER) positive and estrogen-receptor negative subtypes, where ER-negative subtype of breast cancer possess more aggressive behavior, accounting to 25 to 30% of total cases and have poor outcome in the patients relative to other breast cancers, predominantly due to lack of recognized therapeutic molecular targets. The treatment of ER-negative breast cancer patients through effective drug discovery is hence critical (Liu et al., 2019). Bioactive compounds (alkaloids, flavonoids, tannins, terpenoids etc) extracted from natural sources such as plants, animals, algae, fungi play a vital role in anticancer drug discovery and serve as important leads for development of novel therapies (Iqbal et al., 2017, Iqbal et al., 2018c, Batool et al., 2020, Iqbal et al., 2019a, Iqbal et al., 2019b). In scientific community, naturally-derived compounds are gaining substantial attention recently in preventing cancer, cancer therapy, and combatting numerous illnesses (Hashemi, 2015, Zahra et al., 2021a, Zahra et al., 2021b).

Majority of cancer mortality, especially breast cancer mortality occur primarily due to metastasis of primary tumors to different organ sites including brain, liver, bones, lungs, and lymph nodes. Regarding metastatic breast cancer, the 5-year survival rate in patients is calculated to be 25%, suggesting the significance of targeted metastatic therapy (Majumder et al., 2019). Moreover, clinical studies estimated primary tumors to be responsible for only 10% mortality whereas the remaining 90% cancer deaths are due to metastasis alone (Dahham et al., 2016).

Among the different strategies used for preventing cancer, the induction of apoptosis emerges as a promising approach as it is considered one of the most vital characteristic for anti-tumor activity shown by several chemotherapeutic mediators (Sharma et al., 2017). Most apoptotic agents induce apoptosis via either of the two pathways; a receptor-mediated or non-receptor mediated pathway. Evidence accumulated show the apoptosis pathway to be regulated by NF-Kβ, mitogen-activated protein kinases (MAPK), and by GADD (Aggarwal, 2003; Kannaiyan et al., 2011). Owing to the central role of MAPK in cell-proliferation, inflammation, and apoptosis in addition to promotion of apoptosis being the most desirable cancer prevention strategy in neoplastic cells (Lyer

et al., 2008), the current study speculates the P.hydaspidis extract-mediated pro-apoptotic and anti-proliferative effects by modulating MAPK cell-signaling pathway.

Many researchers have previously searched for novel natural products capable of inhibiting the growth of cancerous cells and their proliferation, but at the same time which do not harm normal and hematopoietic cells production. Herbal extracts having antibiotic and anticancer properties have been documented to inhibit the growth and proliferation of cancerous cells with reduced chemotherapeutic drug dosage and ameliorate inherent and severe side-effects (Komonrit and Banjerdpongchai, 2018). One such medicinal plant known for its antimicrobial, anti-inflammatory, hepatoprotective, and antioxidant potential is P. hydaspidis Falc (Ullah et al., 2015; Ali et al., 2018). It belongs to the medicinally important genus "Periploca", which has well-known member's i.e. Periploca aphylla, Periploca sepium, Periploca forestii, Periploca somaliensis, and Periploca laevigata reported for anti-arthritic, anticancer, antioxidant, antimicrobial, wound-healing, and skin treatment potential (Iqbal et al., 2012; Abdel-Monem et al., 2015). Based upon the medicinal worth of P. hydaspidis, the current study investigates its possible anticancer activity using HCCLM3 and MDA-MB 231 cell lines.

2. Materials and methods

2.1. Plant sampling and extract/fraction preparation

The whole plant material of Periploca hydaspidis was collected in the month of April and June 2018 from an elevation of 3600 feet from a mountain located in Charbagh town of District Swat, KPK, Pakistan. The area has four distinct seasons: a spring in March-April, the summer season from May to September, the autumn in October-November, and the winter from December to February. The associated flora predominantly consisted of Dodonaea viscosa, Robinia pseudoacacia, Withania somnifera, Periploca aphylla, Bongardia chrysogonum, Ficus carica, Hedera nepalensis, Rubus fruticosa along with other small herbs and grasses etc. The plant was identified, collected, and confirmed by Dr. Syed Afzal Shah, a plant taxonomist and botanist working in department of Biological Sciences, National University of Medical Sciences, Rawalpindi, Pakistan, Islamabad, Pakistan. A voucher specimen #23651 was placed at Pakistan herbarium, QAU, Isb, Pakistan. The whole plant material (P.hydaspidis) was shade-dried and then converted to fine-textured powder through Willy mill (80 mesh size). This plant powder was thrice (1:8; w/v) extracted with methanol (95%) for extraction of bio-active constituents. The obtained filtrate (PHM) was dried using rotary evaporator. PHM extract (50 g) was suspended in H_2O and the following fractions were acquired in order of escalating polarity by solvent–solvent extraction including n-Hexane (PHH), Ethyl-acetate (PHE), Butanol (PHB), and Aqueous (PHA) fractions. Respective solvents were completely dried from fractions via rotary evaporator and the resultant plant extracts were stored at + 4 °C.

2.2. Reagents used

Sodium dodecyl sulphate (SDS), Tris-glycine, ammonium persulphate (APS), β-mercaptoethanol, EDTA, triton X-100, dulbecco's modified eagle's medium (DMEM), crystal violet dye, trypsin EDTA, ribonuclease A (RNase A), MTT reagent, annexin-V FITC, and propidium iodide (PI) were obtained from sigma-aldrich (St.louis, MO: United states). TEMED, western blot membrane, acrylamide (40%), and laemmli sample buffer were purchased from BIO-Ras (Herculus, CA: United States). Similarly, PBS was acquired from Vivantis technologies (Selangor: Malaysia), fetal bovine serum

(FBS) from Hyclone (Loughborough: United Kingdom), Tween-20 from Merck & Co., Inc, and chemiluminescent substrate for western blot from Advansta (Menlo park, CA: United states). Different antibodies including JNK, p-JNK (Thr183/Tyr185), p38 MAPK, p-p38 MAPK (Thr180/Tyr182), cleaved Caspase-3 (Asp175), cleaved-PARP (Asp214), cleaved Caspase-8 (Asp391), cleaved Caspase-7 (Asp198), Survivin, Cyclin D1, COX-2, XIAP, and β-actin belonged to Cell-Signaling Technology (Massachusetts: U.S.A), whereas, ERK2, p-ERK (Tyr204), Caspase-9, Caspase-3, Caspase-8, BCL-XL, BAX, BAK, MMP9, Cyclin E, C-myc, MMP2, goat anti-mouse antibody-HRP, and goat anti-rabbit antibody-HRP were acquired from Santa-Cruz Biotechnology (Texas: U.S.A).

2.3. Cell lines and culture techniques used

HCCLM3 (human hepatocellular carcinoma) cell line was a gift from Prof. Zhao-You Tang, who works at Liver-Cancer Institute of Zhongshan Hospital (Shanghai, China). MDA-MB 231 (human mammary cancer), MCF-10a (normal mammary epithelial), and LO2 (normal liver) cell lines were obtained from ATCC (American type culture collection). MDA-MB 231, HCCLM3, and LO2 were sub cultured in DMEM (Biowest, Nuaillè, France), whereas MCF-10a was sub cultured in MEGM (mammary epithelial cell-growth medium; Lonza corporation). All culture media's used was supplemented with FBS (10%; Biowest, Nuaillè, France) and penicillin streptomycin (1% of 100X; Thermofisher scientific, U.S.A). Cell lines were kept in humidified incubator provided with 5% CO_2 at + 37 °C.

2.4. Preparation of drug for cell culture

All fractions of P.hydaspidis (80 mg) were suspended in 1 ml of DMSO (dimethyl sulfoxide; sigma–aldrich, U.S.A) to make a stock solution and stored at + 20 °C. Upon use, this stock solution was diluted in culture media as required for different anticancer assays, but maintaining the final concentration of DMSO to be administered below 0.1% during the study course. Similarly, a stock solution of SB239063 (SigmaAldrich, St.louis, USA) in a concentration of 10 mM was prepared in DMSO and stored at + 4 °C. The serial dilutions of SB239063, a pharmacological P38-MAPK inhibitor were prepared in cell culture prior to use following the same procedure as used for plant drugs.

2.5. MTT cell proliferative assay

MTT assay was used to determine the anti-proliferative ability of respective plant formulations post treatment against cancer cell lines. Cancer cells were seeded (10×10^3 cells per well) in triplicates in 96-well plates overnight and were treated with 25, 50, 100, 200, and 400 μg/ml of plant extracts for a time interval of 24, 48, and 72 h. After respective time points, 20 μl MTT (5 mg/ml) was added to each well followed by incubation for 3 h. The medium of well was then replaced by 100 μl DMSO to dissolve formazan crystals. The optical density of each well was recorded at 570 nm by microplate reader (SPARK^{TM} 10 M, TECAN, Switzerland). Cell viability was measured using the equation;

$$Cell\,viability(\%) = \left(\frac{Absorbance\,of\,sample}{Absorbance\,of\,control}\right) \times 100$$

2.6. GC/MS (gas chromatography/mass spectroscopy) analysis

The methanol extract of P.hydaspidis (PHM) was analyzed for the manifestation of active components via GC/MS employing "Thermo GC-Trace Ultra Version: 5.0" gas chromatograph fitted with "Thermo MS DSQ-II"∥ for mass determination. The test sam-

ple components were separated by "Agilent DB-5MS capillary Non-polar Column" having 60 m length and 0.25 μm film thickness. The temperature was raised from 70 to 260 °C throughout the experiment at 06 °C/min frequency. The injection volume of sample to be tested was 1 μl and carrier gas used was helium (1.5 ml/min flowrate). The mass spectra and retention times were matched with authentic samples acquired from NBS/NIST or Wiley Libraries spectra, where the chemical constituents were identified (Cha et al., 2005).

2.7. AV-FITC/PI staining assay

HCCLM3 and MDA-MB 231 cells (0.5 to 0.6×10^6) were seeded in petri-culture dishes (60 mm) overnight after which they were treated with PHM (50, 75, 100, and 150 μg/ml) at 24, 48, and 72 h' interval. The cells treated/untreated with drug were harvested via trypsinization procedure, carefully washed with 1X-PBS (Phosphate Buffered Saline) and finally stained with Annexin V-FITC Kit (Miltenyi Biotech, Bergisch-Gladbach: Germany) for 15–20 min according to manufacturers' protocol. The test samples were then filtered and apoptosis cell percentage was analyzed employing LSR-Fortessa^{TM} flow cytometer (BD-Biosciences, San Diego: U.S.A). All the samples were analyzed within one hour of Annexin-V/PI staining and each trial detected 10,000 events per test sample.

2.8. Cell-cycle arrest analysis assay

HCCLM3 and MDA-MB 231 cells were seeded (0.5 to 0.6×10^6) overnight in cell-culture dishes (60 mm) followed by specified drug (PHM) treatment at 24, 48, and 72 h'. The cells treated were harvested, fixed by ethanol (70%) for half an hour at 4 °C and stored at −20 °C until required. The ethanol-fixed cells were washed following centrifugation and resuspended in 0.5 ml 1X PBS having 1 μl/ml RNase A (Thermo-Fisher Scientific, Waltham: U.S.A) and 7 μl/sample PI (Santa-Cruz Biotechnology, Dallas: U.S.A). After keeping the test samples in dark for 15–20 min, they were filtered and the cell distribution analyzed in various phases of cell-cycle employing LSRFortessa^{TM} flow cytometer (BD-Biosciences, San Diego: U.S.A) and Summit 4.3 software (Beckman-Coulter, Inc.). All samples to be tested were analyzed within one hour of PI staining.

2.9. Wound scratch assay

HCCLM3 and MDA-MB 231 cells were seeded (7×10^4 cells/well) in μ dish-culture inserts (Ibidi-GmbH: Germany) overnight and incubated at 37 °C till the culture flask was confluent. The subsequent day, μ dish-culture inserts were removed straight upward followed by gentle washing with 1X-PBS (1 ml) to create cell-free gap area. The respective cancer cell lines were treated with PHM (50, 100, and 150 μg/ml) and the images were captured using 10X magnification lens at zero, 4, 8, and 12 h' time interval employing Bright-field microscopy (Olympus: DP-70: Japan). The images taken were analyzed through Fiji Software (Schindelin et al., 2012), and normalized wound healed was deliberated using the equation;

$$Normalized\,healed - wound(\%) = \left(\frac{Distance\,of\,closed\,gap\,in\,treated\,\mu\,dishes}{Distance\,of\,closed\,gap\,in\,control\,\mu\,dishes}\right) \times 100$$

2.10. Matrigel invasion analysis assay

The Bio-coat Matrigel invasion chambers (Discovery, Lab-ware Bedford U.S.A) were hydrated and further equilibrated according to manufacturers' protocol. HCCLM3 and MDA-MB 231 cells were

seeded at a density of 7×10^4 cells/well and resuspended in DMEM serum-free media after treatment with indicated PHM concentrations (50, 75, and 100 μg/ml) for 12 h'. FBS (10 %) was added to media and human SDF-1α (CXCL-12) (Prospec Tany-Techno Gene Ltd, NessZiona: Israel) in a concentration of 10 ng/ml was mixed in the lower wells forming a chemotactic-gradient followed by 24 h' incubation period. After indicated treatment and incubation period, the invaded cells were fixed using chilled-methanol (100%) and properly stained with crystal-violet dye (1%). Images were taken using Bright-field microscopy and analyzed via Fiji-Software.

2.11. Western blot analysis

HCCLM3 and MDA-MB 231 cells were seeded (1.3 to 1.7×10^6) overnight in 60 mm cell-culture dishes followed by treatment with indicated drug (PHM) concentration at specified time intervals. The cells treated were harvested and lysed in M−PER (Thermo-Fisher Scientific, Waltham: U.S.A) along with addition of 1% 100X Halt-Protease and Phosphatase Inhibitor Cocktail (Thermo-Fisher Scientific, Waltham: U.S.A) for half an hour placed on ice. The lysates were centrifuged at 13,300 rpm for 15 min to remove any insoluble material if present and the resultant protein was quantified through Bradford protein assay (Sigma-Aldrich, St.louis: U.S.A). Respective lysates were diluted using 4X-Laemmli sample buffer (Bio-Rad Laboratories, California: U.S.A) followed by heating for 5 min at 95 °C for denaturation of protein. The samples processed were stored at −20 °C until required. For gel loading, equivalent amount of protein (30–60 μg) for each sample was resolved onto SDS-PAGE gels (8–10 %) and transferred electrophoretically onto nitrocellulose/PVDF membrane (Bio-Rad Laboratories, California: U.S.A). After transferring, the membrane was blocked with Blocking One (Nasalai-Tesque, Kyoto: Japan) and finally probed with desired primary antibodies at 4 °C overnight. The next day, respective blots were three times washed, incubated in HRP-conjugated (anti-rabbit/anti-mouse) secondary antibody for one hour and subsequently detected via Western-Bright Sirius Chemiluminescent-Detection Kit (Advansta, California: U.S.A). Chemi-Doc Touch Image System (Bio Rad Laboratories, California: U.S.A) was used to take chemiluminescent images. The blots were stripped in Restore™ Stripping buffer (Thermo-Fisher Scientific, Waltham: U.S.A) followed by blocking in blocking buffer, and reprobed with relevant primary antibodies where necessary. Fiji software was used for densitometry analysis.

2.12. Statistical analysis

GraphPad prism-5 software was used for calculating SD, average, IC_{50}, and graphical analyses among different treatment groups at $p \leq 0.001$, $p \leq 0.01$, and $p \leq 0.05$. Fiji (ImageJ) software was functioned for analyzing anticancer assays including Matrigel invasion analysis assay, wound-scratch assay, and performing densitometry analysis of western blot proteins. Apoptosis assay, cell-cycle arrest assay, migration, and invasion data were analyzed by one-way ANOVA trailed by Dunnett's multiple comparison tests, where *, **, *** indicated significance at $p < 0.05$, $p < 0.01$, and $p < 0.001$ relative to control.
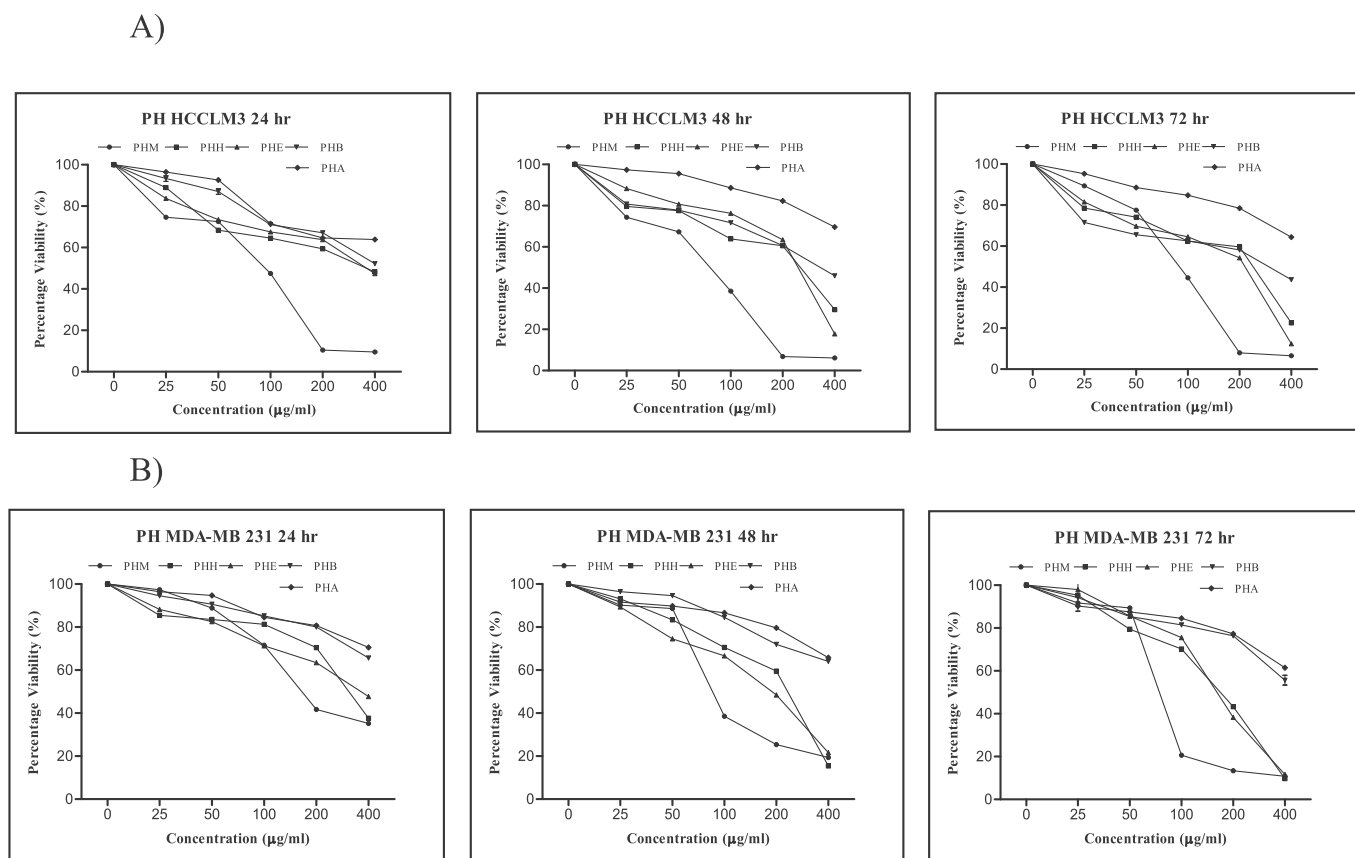

Fig. 1. Anti-proliferative effect of P.hydaspidis fractions against (A) HCCLM3, and (B) MDA-MB 231 cell line at 24, 48, and 72 h. The results are communicated as Mean ± S.D (n = 3) of three independent experiments.

3. Results

3.1. PHM inhibits proliferation of cancer cell lines

PHM fraction of P.hydaspidis revealed maximum anti-proliferative activity alongside all designated cancer cell lines, subject to an increase in dose and time. An IC_{50} of $79.4 ± 0.26$, $67.2 ± 0.70$, and $86.0 ± 0.19$ μg/ml was denoted to PHM against HCCLM3 cells trailed by PHH and PHE ($334 ± 2.70$, $209 ± 1.70$, $176 ± 1.67$ and $393 ± 3.0$, $210 ± 1.88$, $145 ± 0.26$ μg/ml) at 24, 48, and 72 h', respectively (Fig. 1a). Similarly the increasing order of potent anticancer potential alongside MDA-MB231 was drawn as PHA < PHB < PHE < PHH < PHM (Fig. 1b). Only PHM, PHB, and PHE were capable of hindering the proliferation of HEPG2 cells while PHA and PHH showed IC_{50} values exceeding 1000 μg/ml. Significant activity was brought forward by both PHM and PHE alongside MCF-7 corresponding to $199 ± 0.64$, $120 ± 0.92$, $95.8 ± 0.53$ and $440 ± 5.31$, $284 ± 4.07$, $202 ± 2.97$ μg/ml at 24, 48, and 72 h', respectively (supplementary table 1, 2, and 3). Besides this, none of the P.hydaspidis fractions proved cytotoxic to normal cells (liver and breast cell lines; LO2 and MCF-10A).

3.2. GC/MS analysis of PHM

GC/MS of crude methanol extract of P.hydaspidis (PHM) identified a total of 54 compounds conforming to 99.8% of total detected compounds (Table 1). The chromatogram (supplementary Fig. 1) showed evident peaks in the range of 5.51 to 41.3 min. The detected compounds in PHM belonged to 20 major classes including 3 fatty acids (29.8%), 6 benzenoids (15.7%), 11 esters (14.3%), 1 silane (11.3%), 4 alcohols (7.8%), 4 ketones (4.4%), 2 amines (3.2%), 3 aldehydes (3.2%), 1 azole (3.1%), 1 amide (1.5%), 2 tocopherols (1.4%), 2 terpenoids (1.0%), 3 carboxylic acids (0.6%), 4 alkanes (0.6%), 1 anisole (0.4%), 1 benzo-furan (0.4%), 1 alkyne (0.4%), 2 phenols (0.2%), 1 alkene (0.06%) and 1 silicone (0.04%).

3.3. PHM induces apoptosis in HCCLM3 and MDA-MB 231 cells

Apoptosis was induced by PHM as shown in Fig. 2. PHM-induced apoptosis was dependent upon the dose and exposure time used, whereby the ascending order of PHM concentration (50, 75, 100, and 150 μg/ml) increased the apoptotic percentage with an increase in time (24, 48, and 72 h'), respectively. Maximum apoptosis percentage was presented by PHM (150 μg/ml) alongside MDA-MB231 corresponding to $54.8 ± 3.05$, $67.3 ± 3.01$, and $83.50 ± 3.91$ at 24, 48, and 72 h' whereas $32.9 ± 2.5$, $52.20 ± 4.5$, and $72.8 ± 3.45$ was noted for PHM (100 μg/ml) alongside HCCLM3 at equivalent time intervals.

3.4. PHM induced G0/G1 arrest in HCCLM3 and MDA-MB 231 cells

Flow cytometry analysis was done to correlate the anti-proliferative effects of PHM with cell-cycle (G0/G1) arrest at 24, 48, and 72 h', as presented in Fig. 3. The study revealed PHM to induce a concentration and time-dependent apoptosis and cell-cycle growth arrest in HCCLM3 and MDA-MB231 cells. All PHM doses (50, 75, 100, and 150 μg/ml) showed highly significant changes in distribution of cell-cycle population relative to untreated cells. Apoptosis was prompted by all PHM doses as evident from an upsurge in subG1 population and a reduction in G1 cell distribution with passage of time. Maximum subG1 growth arrest was revealed in PHM (150 μg/ml) alongside MDA-MB231 corresponding to 37.2, 69.0, and 89.6% whereas in HCCLM3 cells, the highest cell phase arrest was witnessed by PHM (100 μg/ml) corresponding to 32.9, 50.8, and 69.6% at indicated time intervals.

3.5. PHM suppresses the migration of HCCLM3 and MDA-MB 231 cells

The anti-metastatic potential of PHM was measured in-vitro via wound scratch assay against selected cancer cells (Fig. 4). PHM drug treatment (50, 75, 100, and 150 μg/ml) significantly suppressed (p > 0.001) wound-closure rates relative to untreated. In case of HCCLM3 cells, PHM (100 μg/ml) exhibited wound-closure rates of 1.63, 2.44, and 3.26% compared to untreated showing 18.9, 36.90, and 60.2% at 4, 8, and 12 h'. PHM (150 μg/ml) displayed wound-closure of 0.79, 2.00, and 2.80% in case of MDA-MB231 cells compared to control (26.30, 59.4, and 82.0%) at equivalent time intervals.

3.6. PHM suppresses the invasion of HCCLM3 and MDA-MB 231 cells

Matrigel invasion chambers were used as an in-vitro metastasis model for evaluating anti-metastatic potential of PHM delivered with and without SDF-1 against specified cancer cell lines (Fig. 5). Supplementation with SDF-1 significantly elevated (p > 0.001) cell invasion through matrigel in untreated cells compared to cells not provided with SDF-1. PHM treatment (50, 75, and 100 μg/ml) supplemented with and/or without SDF-1 remarkably decreased the invasive ability relative to untreated cells. Total HCCLM3 invaded cells were quantified as 10.8% and 4.81% in PHM (75 μg/ml) whereas 15.9% and 8.53% of MDA-MB231 cells invaded in PHM (100 μg/ml) delivered with and without SDF-1 relative to untreated (100 %), respectively.

3.7. PHM activates MAPK signaling pathway in HCCLM3 and MDA-MB 231 cells

MAPK's family involves P38 MAPK, JNK, and ERK proteins. Western blot of whole cell-lysates was accomplished to detect alterations in phosphorylated MAPK's levels after drug treatment against HCCLM3 and MDA-MB231 cell lines (Figs. 6a and 7a). The cells were exposed to 8-hour treatment with PHM to detect any early onset changes taking place. Phosphorylated P38 (pP38) MAPK levels noticeably increased time-dependently, where the change was spotted as early as 02 h in HCCLM3 and MDA-MB231 cells. Similarly phosphorylated JNK (pJNK) levels also increased time-dependently, apparent as early as 02 h following PHM treatment in both cell lines. However, the activity of ERK remained unaffected as its protein expressions (pERK and ERK2) stayed the same even after 08 h post treatment. Taken together, the activities of P38 MAPK and JNK were increased following PHM treatment whereas ERK activity remained unaffected.

3.8. P38 MAPK inhibitor studies of PHM

Given that, PHM treatment significantly activated P38 MAPK in western blot analysis within 02 h and that these kinases play regulating roles in apoptosis, the MTT anti-proliferation assay and subG1 flow-cytometer analysis was conducted again but with SB239063 (P38 MAPK Pharmacological inhibitor). This was performed to investigate whether the cyto-toxic and apoptotic effect of PHM was mediated by P38 MAPK activation. Initially, western blotting was done to check the effectiveness of P38 MAPK inhibitor; SB239063 in HCCLM3 and MDA-MB231 cell lines. Figs. 6c and 7c shows pP38 MAPK levels of PHM and SB239063 in-combination to be comparable with control cells as well as considerably lower than PHM-treated cells only. The result suggests the effectiveness of 15 μM and 10 μM SB239063 in suppressing PHM-induced activation of P38 MAPK in HCCLM3 and MDA-MB231 cell lines.

In MTT proliferation assay, PHM treatment (75 and 100 μg/ml) combined with SB239063 considerably reduced the anti-

Table 1
GC/MS analysis of P.hydaspidis crude methanol extract (PHM).

S. No	RT (min)	Compound name*	Chemical Class	Molecular formulae	M. Weight	Area (%)
1	05.51	2-Furancarboxaldehyde, 5-methyl-	Aldehyde	$C_6H_6O_2$	110	0.14
2	09.25	4-Mercaptophenol	Phenol	C_6H_6OS	126	0.16
3	11.14	4H-Pyran-4-one, 2,3-dihydro-3,5-…	Ketone	$C_6H_8O_4$	144	0.14
4	13.37	Benzo furan, 2,3-dihydro-	Benzo-furan	C_8H_8O	120	0.31
5	14.68	Ethanone, 1-(2-hydroxy-5-methylp…	Ketone	$C_9H_{10}O_2$	150	3.07
6	14.92	5-Hydroxymethylfurfural	Aldehyde	$C_6H_6O_3$	126	0.78
7	15.11	5-Hydroxymethylfurfural	Aldehyde	$C_6H_6O_3$	126	1.26
8	15.59	5-Hydroxymethylfurfural	Aldehyde	$C_6H_6O_3$	126	0.94
9	16.88	Benzene, 1-propenyl-	Benzenoid	C_9H_{10}	118	14.48
10	18.21	3-(2-Aminoethyl)-7-methoxyindole	Amine	$C_{11}H_{14}N_2O$	190	2.76
11	19.09	Benzene, 2-propenyl-	Benzenoid	C_9H_{10}	118	0.54
12	20.12	4,7-Dimethoxy-2-methyl-1H-indene	Benzenoid	$C_{12}H_{14}O_2$	190	0.07
13	20.31	2,3,5,6-Tetrafluoroanisole	Anisole	$C_7H_4F_4O$	180	0.44
14	21.02	Phenol, p-(2-nitrovinyl)-	Phenol	$C_8H_7NO_3$	165	0.09
15	21.28	Tricyclo [4.1.0.0(2,4)]heptane, 3…	Alkane	$C_{15}H_{24}$	204	0.14
16	21.98	Benzo furan, 2,3-dihydro-2-methyl…	Benzo-furan	$C_{15}H_{14}O$	210	0.10
17	23.04	1,1-Difluoro-2,2,3-trimethyl-cyc…	Alkane	$C_6H_{10}F_2$	120	0.13
18	23.83	4-Isopropyl-4-methyl-2-phenyl [1,…	Azole	$C_{12}H_{17}BO_2$	204	3.12
19	24.24	Benzene ethanol, .beta.-methyl-4-…	Alcohol	$C_{13}H_{20}O$	192	2.10
20	24.83	Benzene ethanol, .beta.-methyl-4-…	Alcohol	$C_{13}H_{20}O$	192	0.65
21	25.00	Neophytadiene	Terpenoid	$C_{20}H_{38}$	278	0.84
22	25.13	N-(2-Phenylethenyl)acetamide	Amide	$C_{10}H_{11}NO$	161	0.75
23	25.42	9-Octadecyne	Alkyne	$C_{18}H_{34}$	250	0.40
24	25.57	2-Propenoic acid, 3-(2,4-dimetho…	Carb. acid	$C_{11}H_{12}O_4$	208	0.39
25	25.74	11,13-Dimethyl-12-tetradecen-1-o…	Ester	$C_{18}H_{34}O_2$	282	1.16
26	26.19	Benzene, 1-(2-bromoethyl)-4-methyl-	Benzenoid	$C_9H_{11}Br$	198	0.21
27	26.27	Phosphetane, 2,2,3,4,4-pentameth…	Alkane	$C_{11}H_{23}OPS$	234	0.24
28	26.55	Hexadecanoic acid, methyl ester	Ester	$C_{17}H_{34}O_2$	270	1.23
29	26.91	Isophytol	Alcohol	$C_{20}H_{40}O$	296	0.93
30	27.11	3-Pyridinepropanol	Alcohol	$C_8H_{11}NO$	137	0.46
31	27.36	n-Hexadecanoic acid	Fatty acid	$C_{16}H_{32}O_2$	256	5.42
32	27.65	N-(2-Phenylethenyl)acetamide	Amide	$C_{10}H_{11}NO$	161	0.79
33	28.19	Hexadecanoic acid, 14-methyl-, m…	Ester	$C_{18}H_{36}O_2$	284	0.35
34	29.24	8,11-Octadecadienoic acid, methy…	Ester	$C_{19}H_{34}O_2$	294	5.85
35	29.34	9,12,15-Octadecatrienoic acid, m…	Ester	$C_{19}H_{32}O_2$	292	2.26
36	29.67	D-Epi-Inositol, 4-C-methyl-	Alcohol	$C_7H_{14}O_6$	194	3.70
37	29.76	Methyl stearate	Ester	$C_{19}H_{38}O_2$	298	1.73
38	30.18	9,12,15-Octadecatrienoic acid, (…	Fatty acid	$C_{18}H_{30}O_2$	278	19.56
39	30.45	Octadecanoic acid	Fatty acid	$C_{18}H_{36}O_2$	284	4.26
40	30.62	Disilane, ethylpentamethyl-	Silane	$C_7H_{20}Si_2$	160	11.36
41	32.11	Isoindole, 1,3-dihydro-1-imino-2…	Amine	$C_{16}H_{17}N_3$	251	0.48
42	32.34	1-(4-Hydroxy-3-methoxyphenyl) dec…	Ketone	$C_{17}H_{24}O_3$	276	0.83
43	32.71	Eicosanoic acid, methyl ester	Ester	$C_{21}H_{42}O_2$	326	0.32
44	32.90	Oxirane-2-carboxylic acid, 2-ami…	Carb. acid	$C_{10}H_{17}NO_4$	215	0.22
45	33.06	2H-Pyran-2-one, tetrahydro-6-tri…	Ester	$C_{18}H_{34}O_2$	282	0.43
46	33.29	Eicosanoic acid	Fatty acid	$C_{20}H_{40}O_2$	312	0.48
47	34.09	Tridecanoic acid	Fatty acid	$C_{13}H_{26}O_2$	214	0.10
48	34.24	Tetracyclo [4.2.1.0(3,8)0.0(4,7)]n…	Alkene	$C_{12}H_{18}Si$	190	0.06
49	35.08	Octasiloxane, 1,1,3,3,5,5,7,7,9,…	Silicone	$C_{16}H_{50}O_7Si_8$	578	0.04
50	35.21	7-Oxabicyclo [4.1.0] heptane, 1-(2…	Alkane	$C_{15}H_{24}O$	220	0.09
51	35.48	Bis(2-ethylhexyl) phthalate	Ester	$C_{24}H_{38}O_4$	390	0.14
52	35.75	Z-(13,14-Epoxy) tetradec-11-en-1-…	Ester	$C_{16}H_{28}O_3$	268	0.16
53	35.90	Meadow lactone	Ester	$C_{20}H_{38}O_2$	310	0.61
54	36.31	Benzene, 1-phenyl-4-(2-cyano-2-p…	Benzenoid	$C_{21}H_{15}N$	281	0.18
55	37.26	4-((2S,3R)-4-(Benzo[d][1,3] dioxo…	Benzenoid	$C_{20}H_{24}O_4$	328	0.26
56	37.61	Benzaldehyde, 4-methoxy-, (2-nit…	Aldehyde	$C_{14}H_{13}N_3O_3$	271	0.10
57	38.00	1-(4-Hydroxy-3-methoxyphenyl) tet…	Ketone	$C_{21}H_{32}O_3$	332	0.22
58	38.86	Meadow lactone	Ester	$C_{20}H_{38}O_2$	310	0.10
59	39.42	Squalene	Terpenoid	$C_{30}H_{50}$	410	0.20
60	39.94	.alpha.-Tocospiro B	Tocopherol	$C_{29}H_{50}O_4$	462	0.58
61	40.34	.alpha.-Tocospiro B	Tocopherol	$C_{29}H_{50}O_4$	462	0.84
62	40.99	(1,5,5,8-Tetramethyl-bicyclo[4.2…	Carb. acid	$C_{16}H_{28}O_2$	252	0.08
63	41.32	Pyrrolidine-2,5-dione, 1-(2-trif…	Ketone	$C_{18}H_{14}F_3NO_2S$	365	0.17
		Total				99.86

*- Compounds listed in the order of elution from column.

proliferative effects of HCCLM3 cells at 24, 48, and 72 h' compared with PHM alone treatment. Whereas, PHM (50 µg/ml) did not exhibit any differences in cytotoxic effect whether combined with or/ and without SB239063 at any indicated time interval, respectively (Fig. 6d). In case of MDA-MB231 cell line, PHM drug (50, 100, and 150 µg/ml) in-combination with SB239063 markedly decreased the cytotoxic effects at 48 h' relative to PHM treatment given alone as evident in Fig. 7d. Correspondingly, flow cytometry analysis exposed similar results displaying significant reduction in subG1 cell population of HCCLM3 cells after combined treatment of PHM (75, and 100 µg/ml) and SB239063 relative to PHM treatment alone at 48 h'. However, all selected PHM concentrations (50, 100,
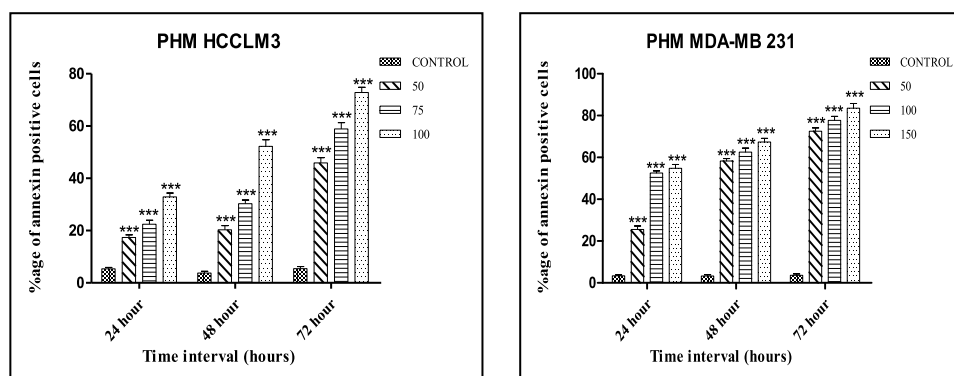
A,B)
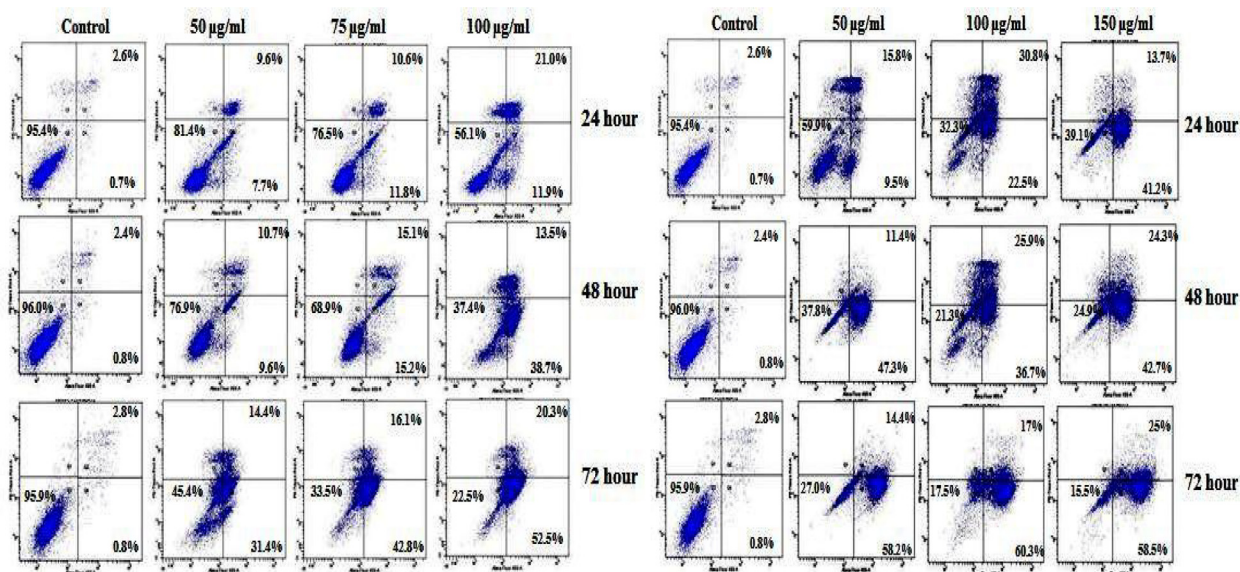
C,D)

Fig. 2. PHM induces apoptosis in (A,B) HCCLM3 and MDA-MB 231 cells, (C,D) Graphical representation of PHM-induced apoptosis in HCCLM3 and MDA-MB 231 cells at 24, 48, and 72 h. The results are communicated as Mean ± S.D (n = 3) and the data was processed by one-way ANOVA followed by Dunnett's multiple-comparison test. *** (significance level at p < 0.001) was noted for PHM concentrations compared to control.

and 150 μg/ml) in-combination with SB239063 clearly reduced the MDA-MB231 cells distribution in subG1 dose-dependently (Fig. 6e and 7e). These outcomes suggest that the anti-proliferative and apoptotic effects were reduced due to PHM-induced activation of P38 MAPK protein, which provides some evidence that the anti-cancer effects of PHM are partially-mediated via P38 MAPK activation.

3.9. PHM regulates anti-metastatic and cell-cycle proteins

Based upon significant roles played by MMP9 and MMP2 proteins in cancer cell migration and invasion, their expression levels were quantified in HCCLM3 and MDA-MB231 cell lines after PHM drug treatment (50, 75, 100, and 150 μg/ml), respectively (Fig. 8a and 9a). The results showed decreased expression of afore-mentioned proteins in a dose-dependent style in both cell lines, signifying PHM to play inhibitory roles in tumor metastasis and its invasion. The main regulators required for cell-cycle progression from G1-S phase including cyclin D1 and cyclin E were quantified to reveal any inhibitory role played following PHM drug treatment against specified cell lines as shown in (Fig. 8a and 9a). The results obtained displayed a reduced protein expression

in a concentration-dependent style in both cell lines, depicting potential inhibitory effects of PHM treatment on cell-cycle progression.

3.10. PHM regulates pro-apoptotic and anti-apoptotic proteins

After flow cytometry analysis, the pro-apoptotic effects of PHM were further demonstrated in HCCLM3 and MDA-MB 231 cells via western blotting analysis involving proteins associated with apoptotic pathway as shown in Figs. 8b and 9b. Main pro-apoptotic proteins (BAX, BAK, Cleaved caspase 8, 9, 3, 7, and PARP) and anti-apoptotic proteins (survivin, BCL-XL, and XIAP) acting antagonistically to each another were detected. Besides this, C-myc levels were also monitored, known for playing significant roles in angiogenesis and tumor growth. The results gained displayed an obvious expression increase in all selected pro-apoptotic proteins whereas an evident decrease in all selected anti-apoptotic proteins was observed dose-dependently. C-myc level was also reduced considerably in both cancer cell lines corresponding to drug dose-dependency. Altogether, the above results match with pro-apoptotic effects of PHM drug as observed earlier in flow-cytometry analysis.
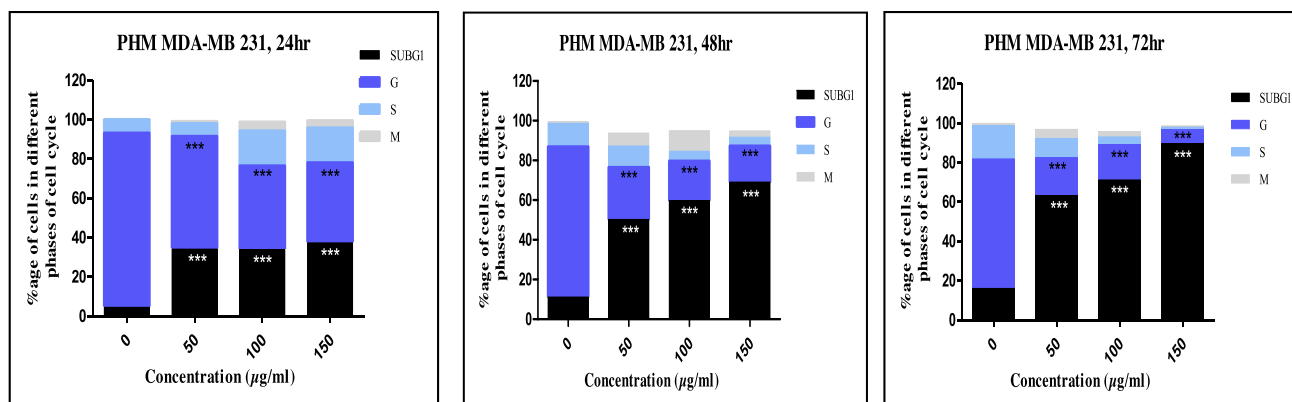
A)
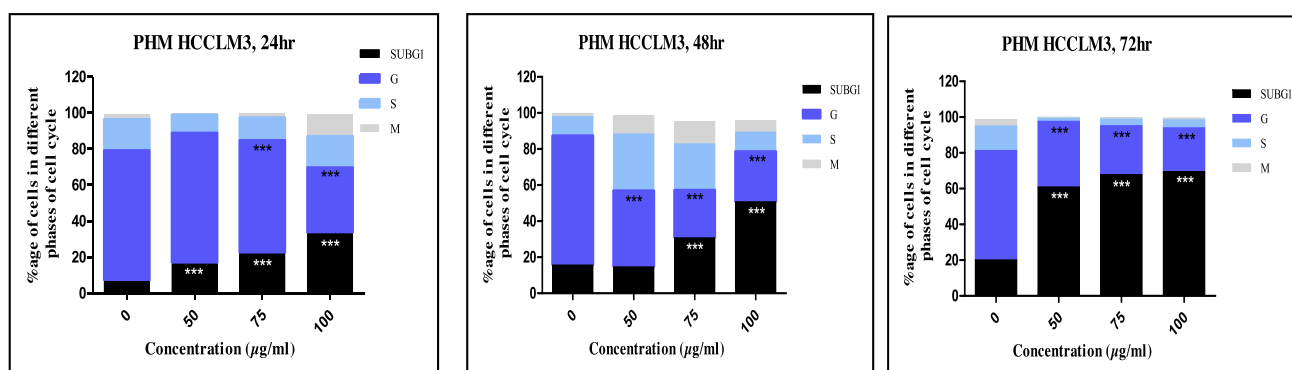
B)

Fig. 3. Cell-cycle arrest analysis of PHM treatment against (A) HCCLM3, (B) MDA-MB 231 cells at 24, 48, and 72 h. The results are communicated as Mean ± S.D (n = 3) and the data was processed one-way ANOVA followed by Dunnett's multiple-comparison test. *** (significance level at p < 0.001) was noted for PHM concentrations at G0/G1 phases of cell-cycle compared to control.

4. Discussion

Natural bio-products are invaluable sources of drug discovery (Guesmi et al., 2018). It is well-documented up till now that medicinal plants serve as a "treasure trove" of bio-active molecules for curing various human illnesses. Uncountable traditional knowledge-based drugs in the previous few decades have been extracted and commercialized. Multiple molecules isolated from medicinal plant origin are presently used as cancer-combating drugs e.g. vinblastine, vincristine, paclitaxel, taxol, and phodophyl-lotoxins) (Majumder et al., 2019). The current investigation reports mechanistic studies of the anticancer activities of P.hydaspidis methanol extract (PHM) via MTT, Annexin-V/PI, G0/G1 phase arrest, migration, invasion, and western blot analysis against HCCLM3 and MDA-MB 231 cell lines.

MTT assay was long developed as the foremost homogenous cell viability assay for 96-well plate format and is highly suitable for high-throughput screening (HTS). This assay has been broadly adopted and remains highly popular in modern research labs as proved by innumerable published research articles (Vinjamuri et al., 2015). The current study involved the initial screening of all fractions of P.hydaspidis against several cancer cell lines i.e. HCCLM3, MCF-7, MDA-MB 231, and HEPG2 via MTT assay. Normal breast (MCF-10A) and liver (LO2) cell lines were also tested parallel in experiment. Considerable cytotoxicity was witnessed against all specified cancer cell lines, particularly PHM, that contributed to the least calculated IC$_{50}$ value among P.hydaspidis fractions. A suitable gap was measured between the IC$_{50}$ values of both normal and cancer cells, signifying cell specificity of plant fractions under study. The capability of drug samples in inhibiting cell-proliferation illustrates the significance of endorsing herbs, shrubs,

and medicinal plants in therapeutics. The inhibitory result of PHM indicated bioactive compounds present that can be potentially used for development of innovative drugs to combat cancer (Sigstedt et al., 2008).

The chemical composition of PHM (P.hydaspidis methanol fraction) was determined via GC/MS analysis. A total of 54 compounds were detected in PHM of which octadecanoic-acid and octadecanoic-acid methyl ester were reported as antibacterial, antifungal, and antitumor agents (Abou-Elela et al., 2009; Hsouna et al., 2011). α-linolenic acid methyl-ester possessed anticancer, antimicrobial, antioxidant, and hyperchloesteralemic activity (Kumar et al., 2010). It has been previously reported to inhibit proliferation of ER-negative and ER-positive breast cancer cells, and is a well-recognized potent anti-angiogenic agent in HUVEC and colorectal cancer cells (Oyugi et al., 2011). 5-Hydroxymethylfurfural containing plants are anti-oxidant and specific anticancer agents (Al-Marzoqi et al., 2016). A triterpenoid; squalene is an antitumour, chemopreventive, cancer preventive, antibacterial, antioxidant, immunostimulant, pesticide, and lipoxygenase-inhibiting agent (Jancy Rani et al., 2011). It serves as a biological precursor of steroids and is active alongside skin, colon, and lung cancers. It is a cytoprotective agent against chemo-therapeutic toxicities (Oyugi et al., 2011).

One of the major strategies emerged for cancer treatment is the induction of cellular-apoptosis (Liu et al., 2019). Researchers define apoptosis as "programmed cell death" which maintains cellular-homeostasis among cell division and death. This physiologic process stimulates cellular self-obliteration and forms different morphological and biochemical changes in the cell nucleus and cytoplasm (Batool et al., 2017). This study establishes the mechanism through which PHM induces apoptosis in HCCLM3 and
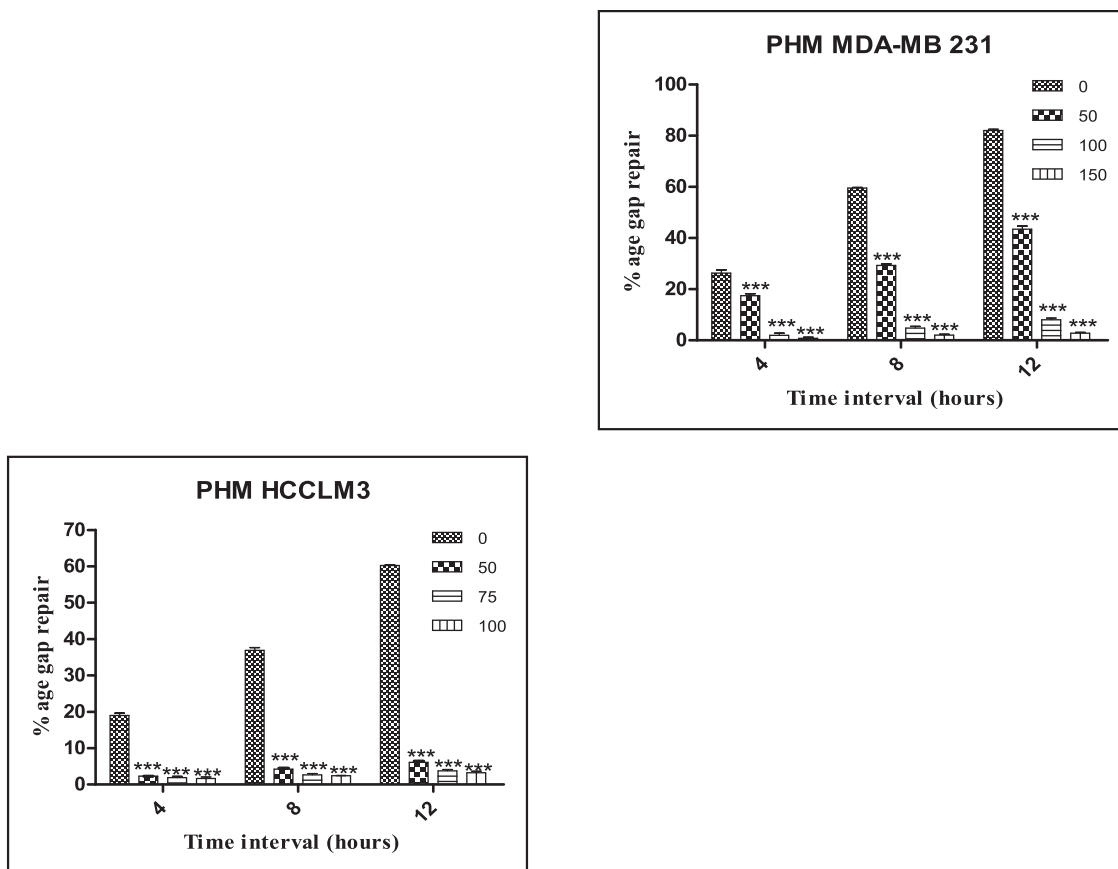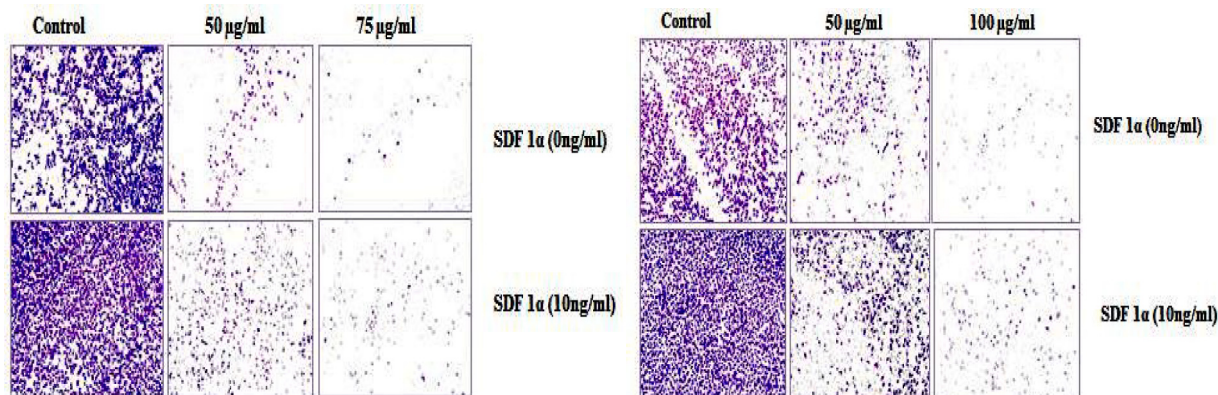
A,B)
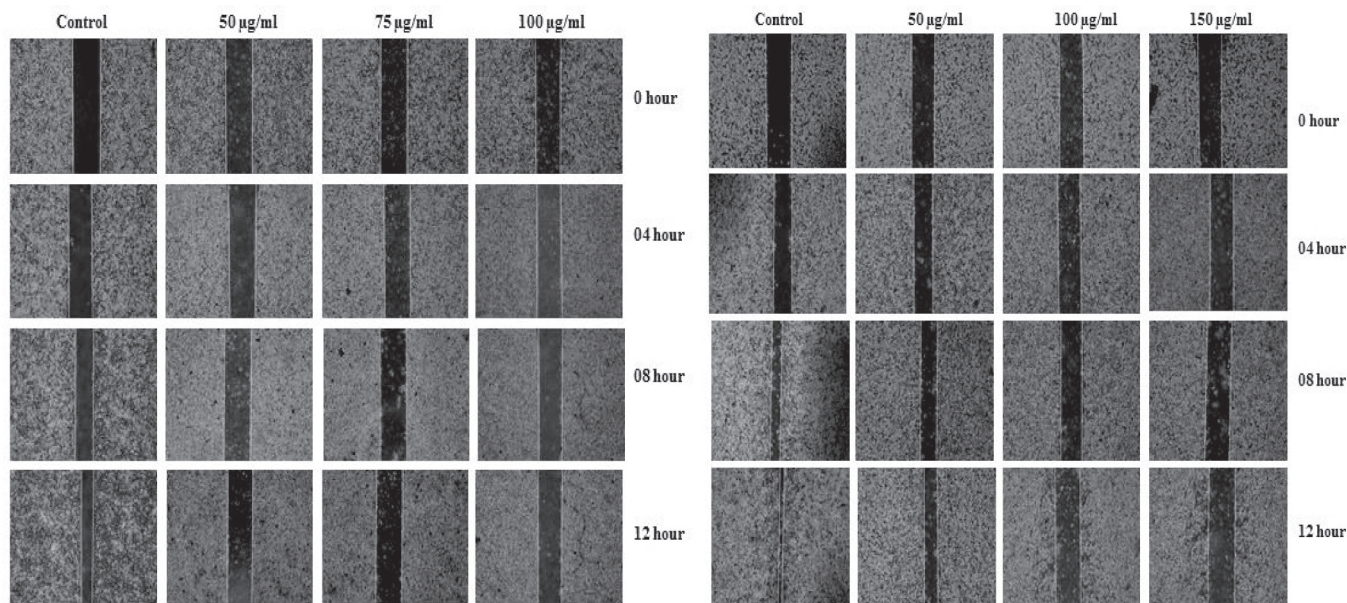
C,D)

Fig. 4. PHM suppressed the migration of (A,B) HCCLM3 and MDA-MB 231 cells, (C,D) Graphical representation showing wound repair (%) of PHM against HCCLM3 and MDA-MB 231 cells at 0, 04, 08, and 12 h. The results are communicated as Mean ± S.D (n = 3) and the data was processed by one-way ANOVA followed by Dunnett's multiple-comparison test. *** (significance level at $p < 0.001$) was noted for PHM concentrations compared to control.
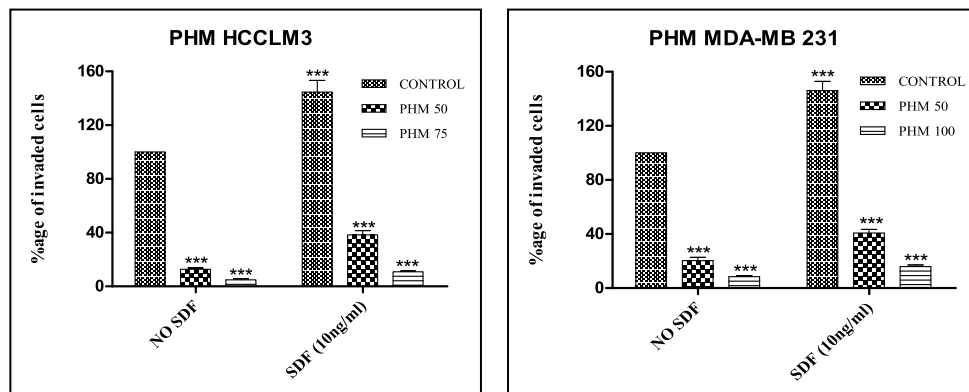
A,B)

C,D)

Fig. 5. PHM suppressed the invasion of (A,B) HCCLM3 and MDA-MB 231 cells, (C,D) Graphical representation of invaded cells (%) following PHM treatment against HCCLM3 and MDA-MB 231 cells at 24 h. The results are communicated as Mean ± S.D (n = 3) and the data was processed by one-way ANOVA followed by Dunnett's multiple-comparison test. *** (significance level at $p < 0.001$) was noted for PHM concentrations compared to control.

MDA-MB 231 cell lines. PHM inhibited cell-proliferation, downregulated cell cycle proteins (cyclin D1 and E), inhibited tumor surviving and promoting proteins (BCL-XL, XIAP, survivin, c-myc), and activated pro-apoptotic proteins (BAK, BAX), and caspases (caspase#3, 7, 8, and 9). PHM increased the number of apoptotic cells in a dose and time-dependent manner in Annexin-V/PI staining assay as well as increased the accumulation of cells in subG1 phase of cell cycle. Cyclin E and cyclin D1 are essentially required by cell-cycle for progression of cells from G1-S phase (Kannaiyan et al., 2011). Consequently, their inhibition blocks the entry of cells to cell cycle and results in their accumulation in subG1 phase. This cell-phase arrest prevents cancer cells to further develop into tumors and also restricts them to spread to new body parts (Qi et al., 2018). Procaspases (9, 8, and 3) and PARP are well-linked with apoptotic cell death pathway (kannaiyan et al., 2011). As soon as caspase-8 and 9 are activated, they start cleaving caspase-3 (Xu et al., 2016). Caspase-3 is involved further in cleaving of various substrates and produce visual alterations and DNA-fragmentation (Goldar et al., 2015). Cleaving of PARP during cell death is also brought forward by caspase-3 (Qi et al., 2018), where PARP-1 itself is a well-designated apoptosis marker and is considered a central target for caspases (Gouthamchandra et al., 2017). Hence, the acti-

vation of caspase −3 and 9 in addition to upregulation of BAX suggest PHM to activate intrinsic apoptosis pathway and encourage cell death through caspase-dependent pathway (Manikandan et al., 2015).

Invasion and metastasis represent the characteristic features of cancerous cells. Local invasion and intra-hepatic metastasis are recognized as the fundamental causes of poor clinical outcomes in HCC patients (Zhang et al., 2017). The current study shows methanol extract of P.hydaspidis (PHM) to inhibit invasion and migration potential of HCCLM3 and MDA-MB 231 cells in a concentration-wise manner. The inhibitory effect of PHM was further validated by western blot analysis, which showed the activity of matrix metalloproteinases (MMP2 and MMP9) to decline considerably post drug treatment. As both MMP2 and MMP9 are well-correlated with tumor formation and metastatic ability of cancerous cells (John and Tuszynski, 2001), therefore their inhibition may open a new therapeutic window for the application of PHM in anti-metastasis therapy.

We also reported the activation of P38 by PHM whereas the suppression of P38 activation by using specific inhibitor (SB239063), which blocked PHM-induced apoptosis. P38 belongs to MAPK family proteins along with others i.e. ERK and JNK. P38

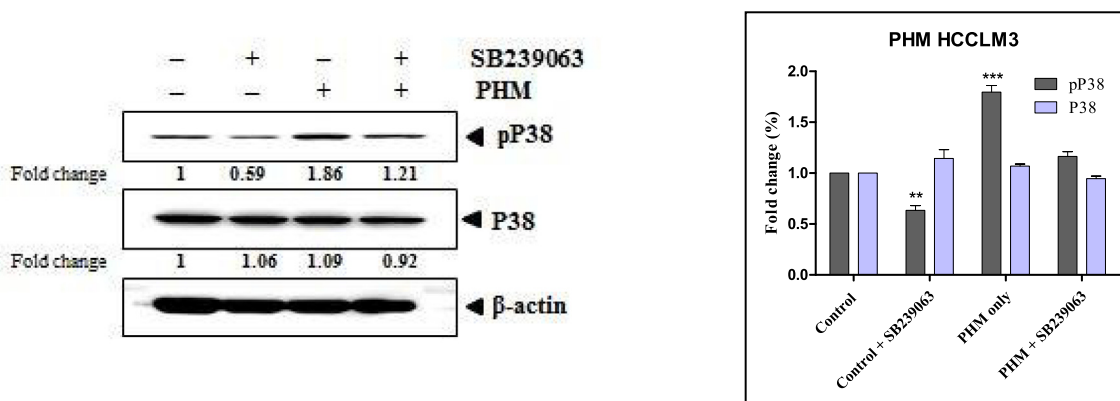**A)**
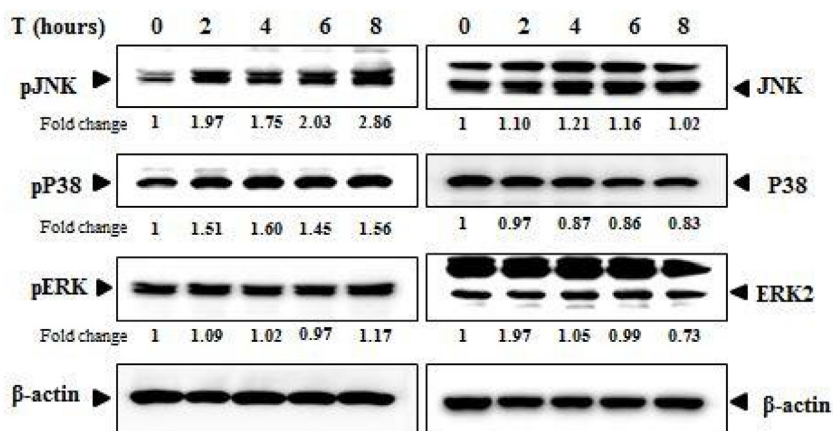
B)
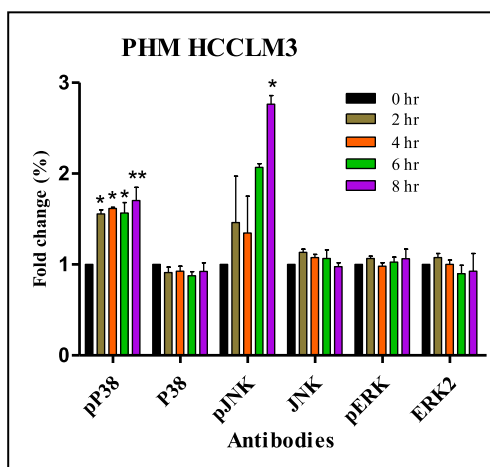
C)

Fig. 6. Western blot analysis showing the effect of PHM on (A) MAPK pathway proteins, (B) graphical representation of PHM treatment against MAPK signaling proteins at 0, 2, 4, 6, and 8 h. (C,D,E) The western blot, MTT, and cell-cycle arrest analysis assays using 15 μM of P38 pharmacological inhibitor (SB239063) against HCCLM3 cells at indicated time intervals. The results are communicated as Mean ± S.D (n = 2) derived from two independent experiments and the data was processed by one-way ANOVA followed Dunnett's multiple-comparison test. *, **, and *** (significance level at $p < 0.05$, $p < 0.01$, $p > 0.001$) was noted for PHM concentrations compared to control.

MAPK cell-signaling pathway is well-implicated in proliferation of a wide-range of cancers (Ding and Chen, 2018). MAPK cell-signaling pathway plays a role in modulation of gene-expression, mitosis, proliferation, metabolism, programmed cell death (Apoptosis), and motility. Both the P38-MAPK's and JNK's are termed stress kinases and their signaling pathways are usually activated concurrently in cancer cells with response to numerous cellular and environmental stresses e.g. changes in osmolarity/metabolism, DNA damage, heat shock, shear stress, ischemia, oxidative stress, UV irradiation ceramide, and inflammatory cytokines (Wada and
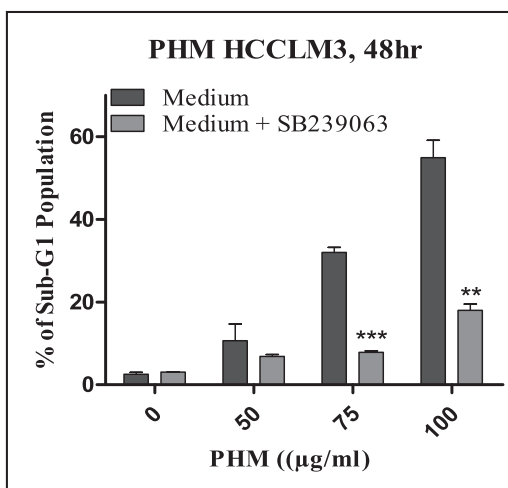
D)
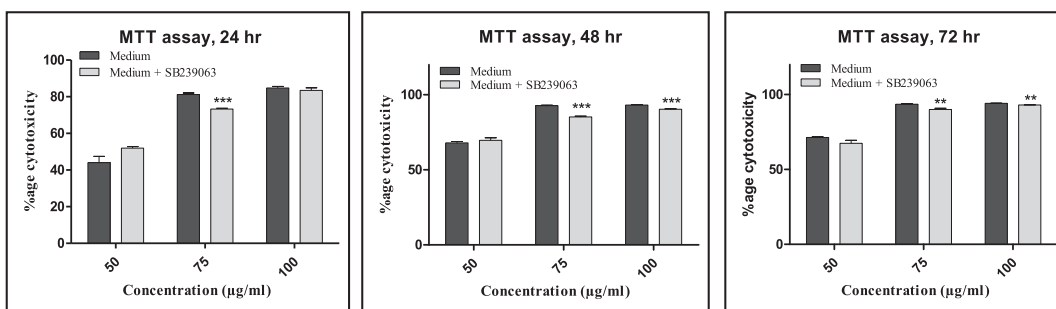
E)

Fig. 6 (*continued*)

Penninger, 2004). Our data proposed the synchronized activation of P38-MAPK and JNK cell-signaling pathway in HCCLM3 and MDA-MB 231 cells with no influence on ERK. As the MAPK's are well-reported to be involved in apoptosis, particularly JNK and P38, therefore it may be projected that PHM instigates apoptosis in HCCLM3 and MDA-MB 231 cells in response to environmental and cellular stress via MAPK cell-signaling pathway. Our experimental results partially agree with Lyer et al., 2008, who reported the pre-treatment with Lactobacillus reuteri to increase JNK and P38 phosphorylation while suppressing ERK 1/2 cell-signaling in TNF-treated KMB5 cells. The authors also suggested P38 MAPK and JNK cell-signaling pathways to exert anta-gonistic effects on ERK signaling, which may serve as an additional mode for regulating apoptosis via enhanced phosphorylation of JNK and P38.

5. Conclusion

Our study demonstrates P.hydaspidis Falc methanol extract (PHM) as the most effective fraction to regulate cell death against HCCLM3 and MDA-MB 231 cancer cell lines of distinctive characteristics. PHM inhibited the aggressiveness of cancer cells via inhibiting metastatic characters including cell motility, adhesion, migration, invasion, and reduced MMP2 and MMP9 protein expressions. Cell cycle arrest was induced in cancer cells, further confirmed by decline in cyclin D1 and cyclin E protein levels. The treatment with PHM induced apoptosis through extrinsic (caspase-8) and intrinsic (caspase-9) pathways by augmenting BAX, resulting in cleavage of caspases particularly cleaved PARP (Fig. 10). This was validated further by cell-signaling studies, where PHM was found to significantly activate the phosphorylation of MAPK family proteins (P38 and JNK) which are involved in apoptotic pathway. Our observations suggest PHM as an important candidate for liver and breast cancer treatment and deserve additional research endeavors. In future, one-step advance studies of PHM regarding its role in metastatic inhibition, immune response modulation for reducing tumor, and inducing apoptosis in suitable animal models would be an interesting and promising research area.
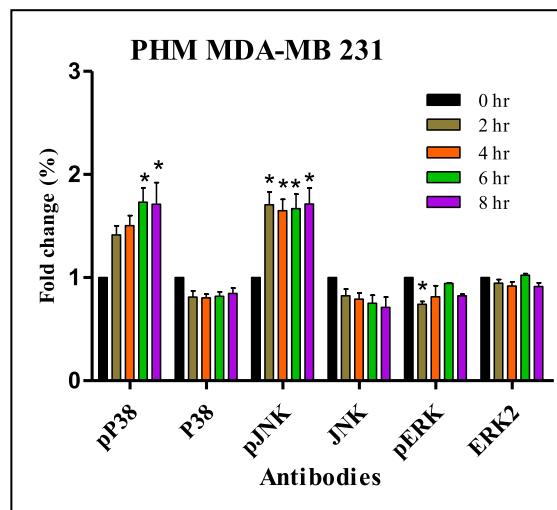
Declaration of Competing Interest

The authors declare that they have no known competing financial interests or personal relationships that could have appeared to influence the work reported in this paper.
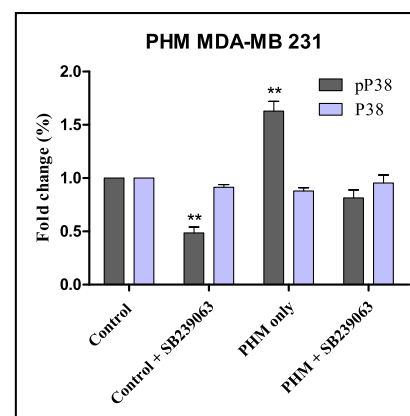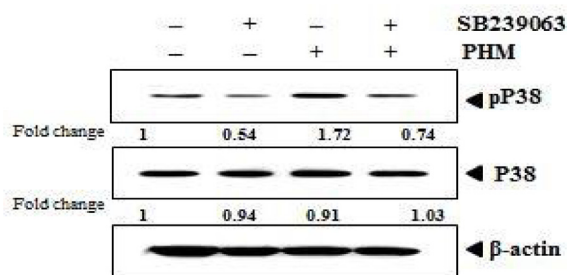
A)
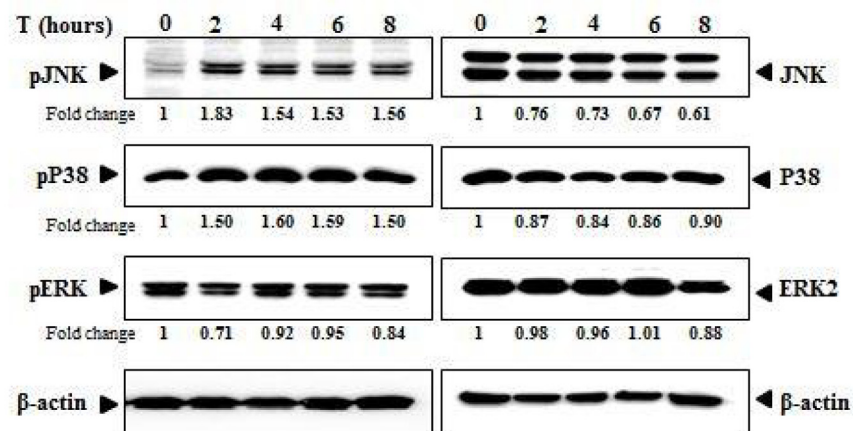
B)

C)

Fig. 7. Western blot analysis showing the effect of PHM on (A) MAPK pathway proteins, (B) graphical representation of PHM treatment against MAPK signaling proteins at 0, 2, 4, 6, and 8 h. (C,D,E) The western blot, MTT, and cell-cycle arrest analysis assays using 10 μM of P38 pharmacological inhibitor (SB239063) against MDA-MB 231 cells at indicated time intervals. The results are communicated as Mean ± S.D (n = 2) derived from two independent experiments and the data was processed by one-way ANOVA followed Dunnett's multiple-comparison test. *, **, and *** (significance level at p < 0.05, p < 0.01, p > 0.001) was noted for PHM concentrations compared to control.
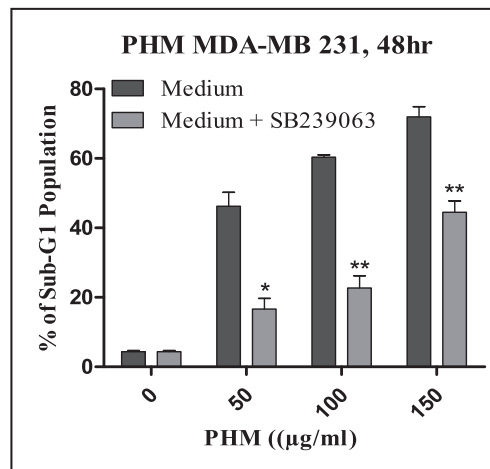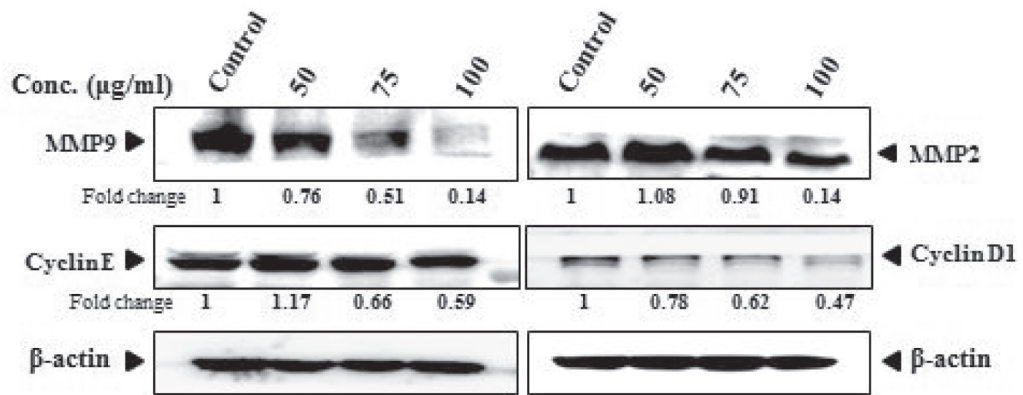
D)
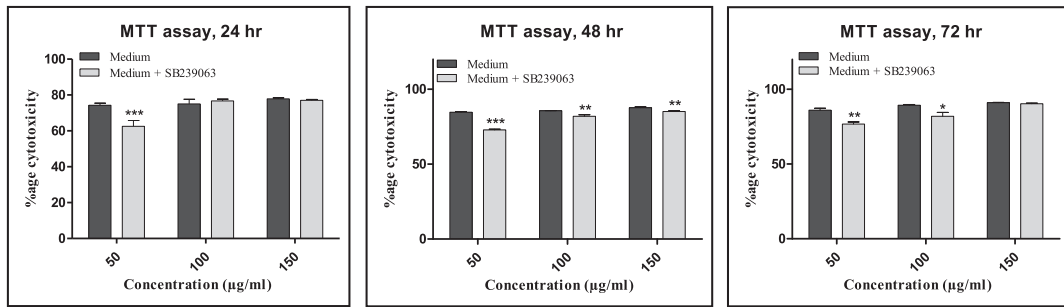
E)

Fig. 7 (*continued*)

Acknowledgements

Appendix A. Supplementary data

Supplementary data to this article can be found online at https://doi.org/10.1016/j.sjbs.2021.08.020.
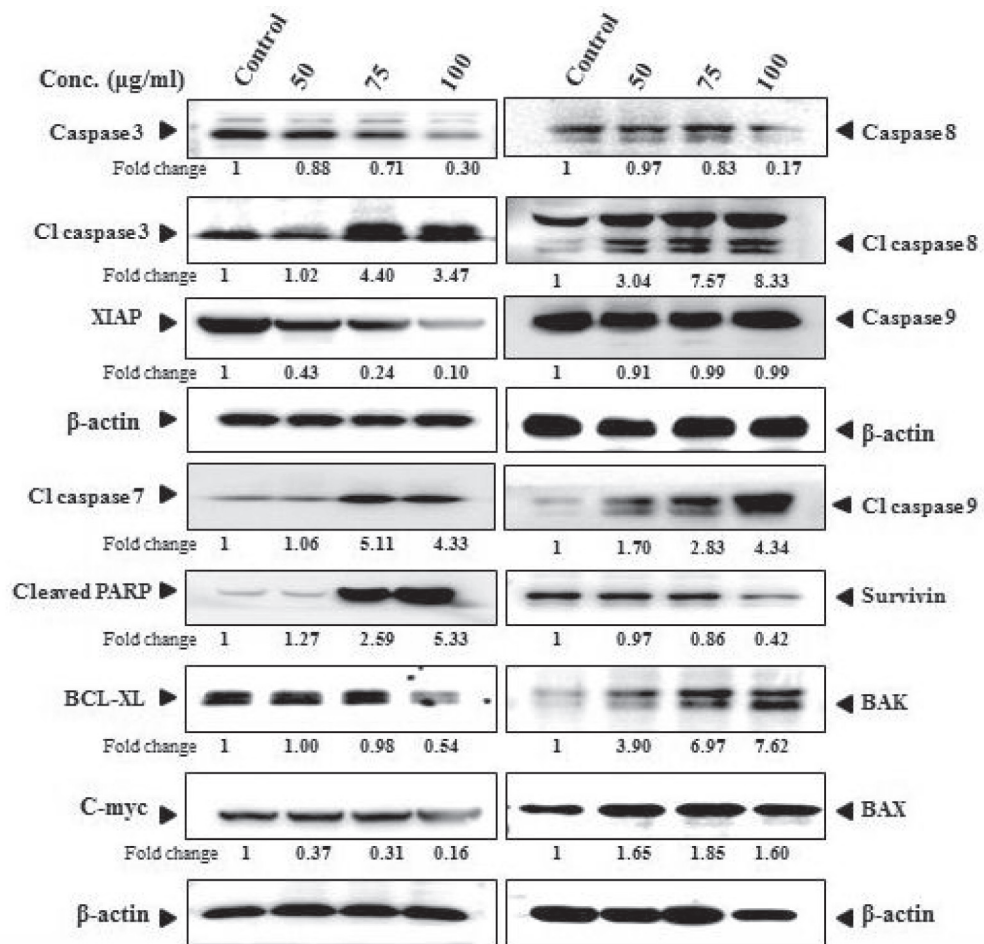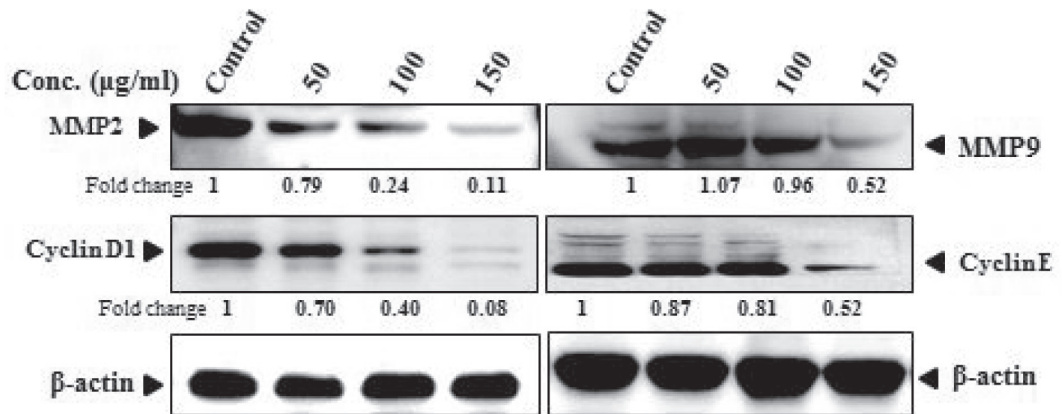
A)

B)

Fig. 8. Western blot analysis showing the effect of PHM on (A) Metastatic and cell-cycle proteins (B) pro-apoptotic and anti-apoptotic proteins against HCCLM3 cell line. HCCLM3 cells were treated with 50, 75, and 100 μg/ml at 24, 48, and 72 h. Proteins were equally loaded onto the wells, also confirmed by β-actin loading control. Fold change was calculated using Fiji ImageJ software.
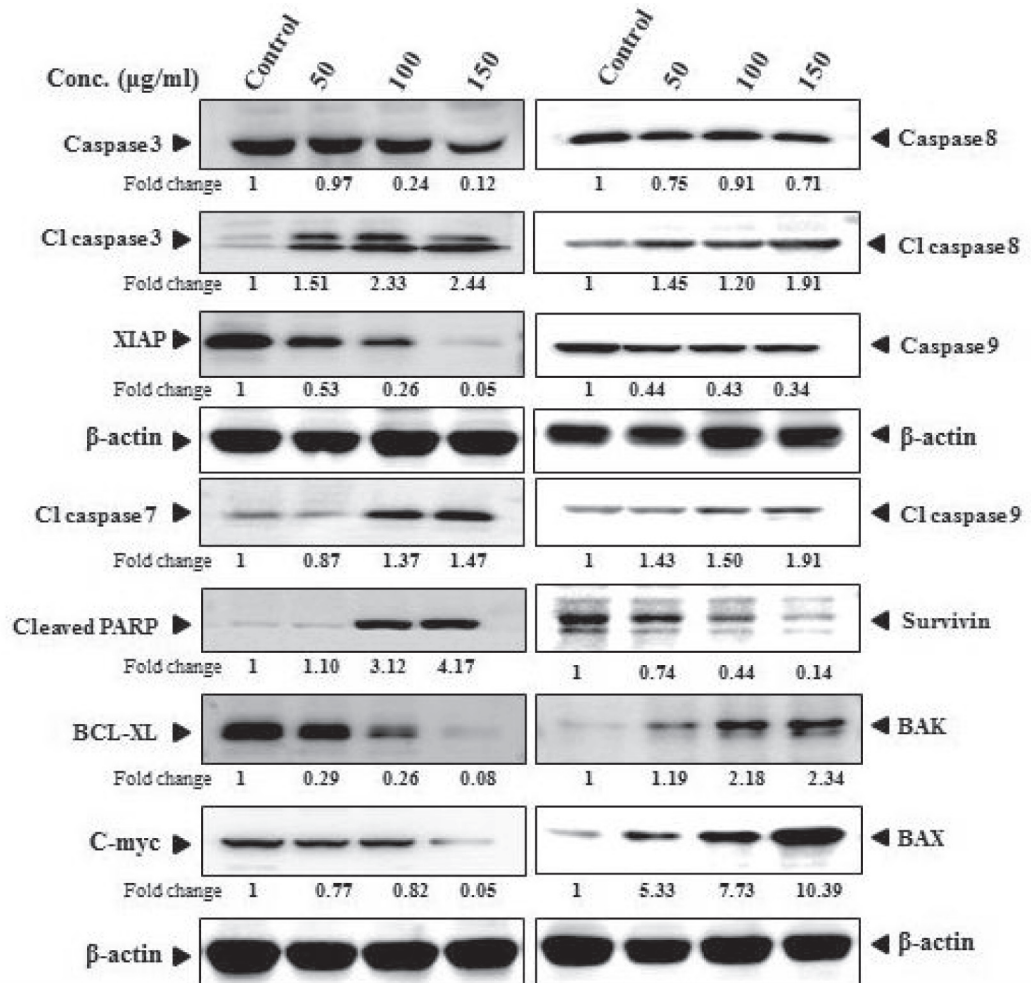
A)

B)

Fig. 9. Western blot analysis showing the effect of PHM on (A) Metastatic and cell-cycle proteins (B) pro-apoptotic and anti-apoptotic proteins against MDA-MB 231 cell line. MDA-MB 231 cells were treated with 50, 75, and 100 μg/ml at 24, 48, and 72 h. Proteins were equally loaded onto the wells, also confirmed by β-actin loading control. Fold change was calculated using Fiji ImageJ software.
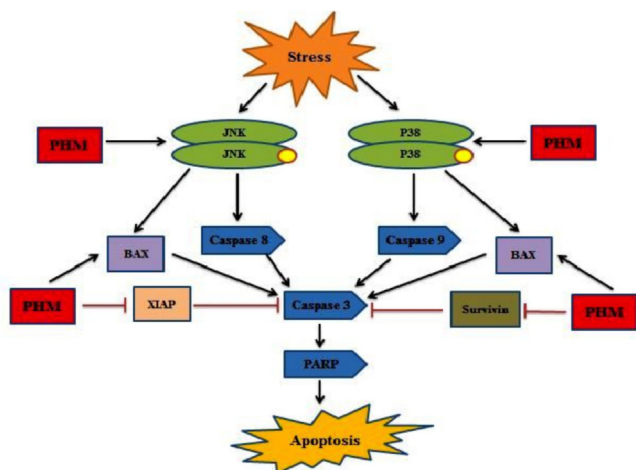
Fig. 10. Proposed anticancer mechanism of PHM. indicates activation, indicates inhibition, indicates phosphorylation, is effective extract/compound against HCCLM3 and MDA-MB 231 cell lines.

References

Abdel-Monem, A.R., Kandil, Z.A., Abdel-Naim, A.B., Abdel-Sattar, E., 2015. A new triterpene and protective effect of Periploca somaliensis Browicz fruits against CCl4-induced injury on human hepatoma cell line (Huh7). Nat. Prod. Res. 29, 423–429.

Abou-Elela, G.M., Abd-Elnaby, H., Ibrahim, H.A., Okbah, M., 2009. Marine natural products and their potential applications as anti-infective agents. World Appl. Sci. J. 7, 872–880.

Abbasi, B.A., Iqbal, J., Mahmood, T., Khalil, A.T., Ali, B., Kanwal, S., Ahmad, R., 2018. Role of dietary phytochemicals in modulation of miRNA expression: Natural swords combating breast cancer. Asian Pac. J. Trop. Med. 11, 501–509.

Abbasi, B.A., Iqbal, J., Ahmad, R., Bibi, S., Mahmood, T., Kanwal, S., Hameed, S., 2019. Potential phytochemicals in the prevention and treatment of esophagus cancer: A green therapeutic approach. Pharmacol. Rep. 71, 644–652.

Abbasi, B.A., Iqbal, J., Kiran, F., Ahmad, R., Kanwal, S., Munir, A., Mahmood, T., 2020. Green formulation and chemical characterizations of Rhamnella gilgitica aqueous leaves extract conjugated NiONPs and their multiple therapeutic properties. J. Mol. Struct. 1218, 128490.

Abbasi, B.A., Iqbal, J., Nasir, J.A., Zahra, S.A., Shahbaz, A., Uddin, S., Mahmood, T., 2020b. Environmentally friendly green approach for the fabrication of silver oxide nanoparticles: Characterization and diverse biomedical applications. Microsc. Res. Tech. 83, 1308–1320.

Abbasi, B.A., Iqbal, J., Zahra, S.A., Shahbaz, A., Kanwal, S., Rabbani, A., Mahmood, T., 2020d. Bioinspired synthesis and activity characterization of iron oxide nanoparticles made using Rhamnus Triquetra leaf extract. Mater. Res. Express 6, 1250e7.

Abbasi, B.A., Iqbal, J., Khan, Z., Ahmad, R., Uddin, S., Shahbaz, A., Mahmood, T., 2021. Phytofabrication of cobalt oxide nanoparticles from Rhamnus virgata leaves extract and investigation of different bioactivities. Microsc. Res. Tech. 84, 192–201.

Aggarwal, B.B., 2003. Signalling pathways of the TNF superfamily: a double-edged sword. Nat. Rev. Immunol. 3, 745–756.

Ali, S., Khan, M.R., Shah, S.A., Batool, R., Maryam, S., Majid, M., Zahra, Z., 2018. Protective aptitude of Periploca hydaspidis Falc against CCl4 induced hepatotoxicity in experimental rats. Biomed. 105, 1117–1132.

Al-Marzoqi, A.H., Hadi, M.Y., Hameed, I.H., 2016. Determination of metabolites products by Cassia angustifolia and evaluate antimicobial activity. J. Pharmacogn. Phytotherapy 8, 25–48.

Batool, R., Aziz, E., Tan, B.-K.-H., Mahmood, T., 2017. Rumex dentatus inhibits cell proliferation, arrests cell cycle, and induces apoptosis in MDA-MB-231 cells through suppression of the NF-κB pathway. Front. Pharmacol. 8, 731.

Batool, R., Aziz, E., Salahuddin, H., Iqbal, J., Tabassum, S., Mahmood, T., 2019. Rumex dentatus could be a potent alternative to treatment of micro-bial infections and of breast cancer. J. Tradit. Chin. Med. 39, 772–779.

Batool, R., Aziz, E., Iqbal, J., Salahuddin, H., Tan, B.K.H., Tabassum, S., Mahmood, T., 2020. In vitro antioxidant and anti-cancer activities and phytochemical analysis of Commelina benghalensis L. root extracts. Asian Pac. J Trop. Biomed. 10, 417.

Cha, J.D., Jeong, M.R., Jeong, S.I., Moon, S.E., Kim, J.Y., Kil, B.B.S., 2005. Chemical composition and antimicrobial activity of the essential oils of Artemisia scoparia and A. capillaris. Planta Med. 71, 186–190.

Dahham, S.S., Tabana, Y.M., Hassan, L.E.A., Ahamed, M.B.K., Majid, A.S.A., Majid, A.M.S.A., 2016. In vitro antimetastatic activity of Agarwood (Aquilaria crassna) essential oils against pancreatic cancer cells. Alexandria J. Med. 52, 141–150.

Ding, X., Chen, H., 2018. Anticancer effects of Carvone in myeloma cells is mediated through the inhibition of p38 MAPK signalling pathway, apoptosis induction and inhibition of cell invasion. J. Buon 23, 747–751.

Goldar, S., Khaniani, M.S., Derakhshan, S.M., Baradaran, B., 2015. Molecular mechanisms of apoptosis and roles in cancer development and treatment. Asian Pac. J. Cancer Prev. 16, 2129–2144.

Gouthamchandra, K., Sudeep, H., Venkatesh, B., Prasad, K.S., 2017. Chlorogenic acid complex (CGA7), standardized extract from green coffee beans exerts anticancer effects against cultured human colon cancer HCT-116 cells. Food Sci. Hum. Well. 6, 147–153.

Guesmi, F., Tyagi, A.K., Prasad, S., Landoulsi, A., 2018. Terpenes from essential oils and hydrolate of Teucrium alopecurus triggered apoptotic events dependent on caspases activation and PARP cleavage in human colon cancer cells through decreased protein expressions. Oncotarget 9, 32305.

Hashemi, J.M., 2015. Protective Effect of Curcumin on Hepatocarcinoma induced by N-Nitrosodiethylamine in Male Rats. Nat. Sci. 13, 117–126.

Hsouna, A.B., Trigui, M., Mansour, R.B., Jarraya, R.M., Damak, M., Jaoua, S., 2011. Chemical composition, cytotoxicity effect and antimicrobial activity of Ceratonia siliqua essential oil with preservative effects against Listeria inoculated in minced beef meat. Int. J. Food Microbiol. 148, 66–72.

Iqbal, J., Zaib, S., Farooq, U., Khan, A., Bibi, I., Suleman, S., 2012. Antioxidant, antimicrobial, and free radical scavenging potential of aerial parts of Periploca aphylla and Ricinus communis. ISRN. Pharmacology.

Iqbal, J., Abbasi, B.A., Mahmood, T., Kanwal, S., Ali, B., Shah, S.A., Khalil, A.T., 2017. Plant-derived anticancer agents: A green anticancer approach. Asian Pac. J. Trop. Biomed. 7, 1129–1150.

Iqbal, J., Abbasi, B.A., Ahmad, R., Mahmood, T., Kanwal, S., Ali, B., Badshah, H., 2018a. Ursolic acid a promising candidate in the therapeutics of breast cancer: Current status and future implications. Biomed. Pharmacother. 108, 752–756.

Iqbal, J., Abbasi, B.A., Batool, R., Mahmood, T., Ali, B., Khalil, A.T., Ahmad, R., 2018b. Potential phytocompounds for developing breast cancer therapeutics: nature's healing touch. Eur. J. Pharmacol. 827, 125–148.

Iqbal, J., Abbasi, B.A., Khalil, A.T., Ali, B., Mahmood, T., Kanwal, S., Ali, W., 2018c. Dietary isoflavones, the modulator of breast carcinogenesis: Current landscape and future perspectives. Asian Pac. J. Trop. Med. 11, 186–193.

Iqbal, J., Abbasi, B.A., Ahmad, R., Batool, R., Mahmood, T., Ali, B., Munir, A., 2019a. Potential phytochemicals in the fight against skin cancer: Current landscape and future perspectives. Biomed. Pharmacother. 109, 1381–1393.

Iqbal, J., Shinwari, Z.K., Mahmood, T., 2019b. Phylogenetic relationships within the cosmopolitan family rhamnaceae using atpB gene promoter. Pak. J. Bot. 51, 1027–1040.

Iyer, C., Kosters, A., Sethi, G., Kunnumakkara, A.B., Aggarwal, B.B., Versalovic, J., 2008. Probiotic Lactobacillus reuteri promotes TNF-induced apoptosis in human myeloid leukemia-derived cells by modulation of NF-κB and MAPK signalling. Cell. Microbiol. 10, 1442–1452.

Jancy Rani, P.M., Kannan, P., Kumaravel, S., 2011. Screening of antioxidant activity, total phenolics and gas chromatograph and mass spectrometer (GC-MS) study of Delonix regia. Afr. J. Biochem. Res. 2, 341–347.

John, A., Tuszynski, G., 2001. The role of matrix metalloproteinases in tumor angiogenesis and tumor metastasis. Pathol. Oncol. Res. 7, 14.

Kannaiyan, R., Manu, K.A., Chen, L., Li, F., Rajendran, P., Subramaniam, A., Lam, P., Kumar, A.P., Sethi, G., 2011. Celastrol inhibits tumor cell proliferation and promotes apoptosis through the activation of c-Jun N-terminal kinase and suppression of PI3 K/Akt signaling pathways. Apoptosis 16, 1028.

Komonrit, P., and Banjerdpongchai, R., 2018. Effect of Pseuderanthemum palatiferum (Nees) Radlk fresh leaf ethanolic extract on human breast cancer MDA-MB-231 regulated cell death. Tumor Biol. 40, 1010428318800182.

Kumar, P.P., Kumaravel, S., Lalitha, C., 2010. Screening of antioxidant activity, total phenolics and GC-MS study of Vitex negundo. Afr. J. Biochem. Res. 4, 191–195.

Liu, L., Ahn, K.S., Shanmugam, M.K., Wang, H., Shen, H., Arfuso, F., Chinnathambi, A., Alharbi, S.A., Chang, Y., Sethi, G., 2019. Oleuropein induces apoptosis via abrogating NF-κB activation cascade in estrogen receptor–negative breast cancer cells. J. Cell. Biochem. 120, 4504–4513.

Majumder, M., Debnath, S., Gajbhiye, R.L., Saikia, R., Gogoi, B., Samanta, S.K., Das, D.K., Biswas, K., Jaisankar, P., Mukhopadhyay, R., 2019. Ricinus communis L. fruit extract inhibits migration/invasion, induces apoptosis in breast cancer cells and arrests tumor progression in vivo. Sci. Rep-UK 9, 1–14.

Manikandan, R., Manikandan, B., Raman, T., Arunagirinathan, K., Prabhu, N.M., Basu, M.J., Perumal, M., Palanisamy, S., Munusamy, A., 2015. Biosynthesis of silver nanoparticles using ethanolic petals extract of Rosa indica and characterization of its antibacterial, anticancer and anti-inflammatory activities. Spectrochimica Acta A. 138, 120–129.

Najmuddin, S.U.F.S., Romli, M.F., Hamid, M., Alitheen, N.B., Rahman, N.M.A.N.A., 2016. Anti-cancer effect of Annona Muricata Linn Leaves Crude Extract (AMCE) on breast cancer cell line. BMC Complem. Altern. M. 16, 311.

Oyugi, D.A., Ayorinde, F.O., Gugssa, A., Allen, A., Izevbigie, E.B., Eribo, B., Anderson, W.A., 2011. Biological activity and mass spectrometric analysis of Vernonia amygdalina fractions. J. Biosci. Tech. 2, 287–304.

Qi, F., Yan, Q., Zheng, Z., Liu, J., Chen, Y., Zhang, G., 2018. Geraniol and geranyl acetate induce potent anticancer effects in colon cancer Colo-205 cells by inducing apoptosis, DNA damage and cell cycle arrest. J. Buon 23, 346–352.

Schindelin, J., Arganda-carreras, I., Frise, E., Kaynig, V., Longair, M., Pietzsch, T., Cardona, A., 2012. Fiji : an open-source platform for biological-image analysis. Nat. Methods 9 (7), 676–682.

Sharma, R., Kaushik, S., Shyam, H., Agarwal, S., Balapure, A.K., 2017. Neem seed oil induces apoptosis in MCF-7 and MDA MB-231 human breast cancer cells. Asian Pac. J. Cancer P: APJCP. 18, 2135.

Sigstedt, S.C., Hooten, C.J., Callewaert, M.C., Jenkins, A.R., Romero, A.E., Pullin, M.J., Kornienko, A., Lowrey, T.K., Slambrouck, S.V., Steelant, W.F., 2008. Evaluation of

aqueous extracts of Taraxacum officinale on growth and invasion of breast and prostate cancer cells. Int. J. Oncol. 32, 1085–1090.

Stewart, B.W., Wild, C., 2014. Word cancer report 2014. Nonserial Publication, IARC.

Sung, H., Ferlay, J., Siegel, R.L., Laversanne, M., Soerjomataram, I., Jemal, A., Bray, F., 2021. Global cancer statistics 2020: GLOBOCAN estimates of incidence and mortality worldwide for 36 cancers in 185 countries. CA: Cancer. J. Clin. 71, 209–249.

Ullah, R., Bakht, J., Shafi, M., 2015. Antimicrobial and anti-oxidant potential of Periploca hydaspidis. Bangl. J. Pharmacol. 10, 645–651.

Vinjamuri, S., Shanker, D., Ramesh, R.S., Nagarajan, S., 2015. In vitro evaluation of hemolytic activity and cell viability assay of hexanoic extracts of Bridelia ferruginea benth. World J. Pharm. Pharm. Sci. 4, 1263–1268.

Wada, T., Penninger, J.M., 2004. Mitogen-activated protein kinases in apoptosis regulation. Oncogene 23, 2838.

Xu, G., Kuang, G., Jiang, W., Jiang, R., Jiang, D., 2016. Polydatin promotes apoptosis through upregulation the ratio of Bax/Bcl-2 and inhibits proliferation by attenuating the β-catenin signaling in human osteosarcoma cells. Am. J. Transl. Res. 8, 922.

Zhang, W., Qian, S., Yang, G., Zhu, L., Zhou, B., Liu, R., Qu, X., Wang, J., Yan, Z., 2017. MicroRNA-519 suppresses cell growth and invasion by reducing HuR levels in hepatocellular carcinoma. Int. J. Clin. Exp. Pathol. 10, 6415–6424.

Zahra, S.A., Iqbal, J., Abbasi, B.A., Shahbaz, A., Kanwal, S., Shah, S.L., Mahmood, T., 2021a. Antimicrobial, cytotoxic, antioxidants, enzyme inhibition activities, and scanning electron microscopy of Lactuca orientalis (Boiss.) Boiss. Seeds. Microsc Res Tech 84, 1284–1295.

Zahra, S.A., Iqbal, J., Abbasi, B.A., Yaseen, T., Hameed, A., Shahbaz, A., Ahmad, P., 2021b. Scanning electron microscopy of Sophora alopecuroides L. seeds and their cytotoxic, antimicrobial, antioxidant, and enzyme inhibition potentials. Microsc. Res. Tech.